Nuclear Physics News

Nuclear Physics News is published on behalf of the Nuclear Physics European Collaboration Committee (NuPECC), an Expert Committee of the European Science Foundation, with colleagues from Europe, America, and Asia.

Volume 14/No. 4

Editorial Office: Physikdepartment, E12, Technische Universitat München,
85748 Garching, Germany, Tel: +49 89 2891 2293, +49 172 89 15011, Fax: +49 89 2891 2298,
E-mail: sissy.koerner@ph.tum.de

Nuclear Physics News ISSN 1050-6896

Advertising Manager
Maureen M. Williams, P.O. Box 1547
Surprise, AZ 85378-1547, USA
Tel: +1 623 544 1698
Fax: +1 623 544 1699
E-mail: mwilliams@cisaz.com

Circulation and Subscriptions
Taylor & Francis Inc.
325 Chestnut Street
8th Floor
Philadelphia, PA 19106, USA
Tel: +1 215 625 8900
Fax: +1 215 625 8914

Subscriptions
Nuclear Physics News is supplied free of charge to nuclear physicists from contributing countries upon request. In addition, the following subscriptions are available:

Volume 14(2004), 4 issues
Personal: $57 USD, £35 GBP
Institution: $461 USD, £279 GBP

Nuclear Physics News

Volume 14/No. 4

Contents

Cover illustration: Upper end of the chart of nuclei showing the presently known nuclei in colors attributed to their decay mode: α decay yellow, β^+ decay red, β^- decay blue, spontaneous fission green, and γ decaying isomers white. Also given are the measured half-lives and α-decay chains observed in experiments. The background structure in blue color shows the calculated shell correction energy according to the macroscopic-microscopic model with minimum values of –7 MeV (darkest blue) for both deformed nuclei at Z = 108, N = 162 and spherical superheavy nuclei at Z = 114, N = 184. The intensity of the blue color is reduced with increasing shell correction energy in steps of 1 MeV.

To Publish or Not to Publish in Proceedings?

That is indeed the question that is on my mind when returning from a workshop or a conference. This might seem strange at first sight, but the question is triggered by the fact that more and more conference proceedings appear in regular scientific journals and that lately new research evaluation criteria appear. One of the arguments often used in favor of refereed conference proceedings is that it gives more possibilities for PhD students to become first author on a publication in a refereed journal. This is a false argument and in the long term the tendency of publishing conference proceedings in regular journals will hurt our field.

Nowadays different criteria are used to evaluate research projects. These evaluation processes are important not the least for society that has the right to know if the resources it invests in fundamental research—even though they are scarce—are well spent. It is however difficult to measure the quality of fundamental research projects as its real quality can often only be judged after a long time. A way out, that has become common practice, is to combine measurable quantities with reports from peer reviewing, with strategic plans and with a lot of common sense. One such measurable parameter is related to the publications; indeed one of the most relevant outputs of our research. Counting the number of publications, the number of papers as first, second, or last author, the number of citations as well as the impact factor of the journals has become a commercial activity and it is thus easy to get all the numbers. Companies, for example, ISI web of knowledge, not only deliver these results but also define the parameters (impact factors, number of citations versus world averages, etc.) and categorize the journals in different research domains. The definition of the parameters is out of control of the research groups and evaluation committees tend to use criteria that sometimes do not make sense. Furthermore, when the evaluation deals with projects or candidates from different research fields the measurable quantities gain more and more importance. In the long term all of this will be devastating for our research funding. Let me illustrate this with a few examples.

In our field there are no standard rules for the order of the author list available and if they exist they definitely differ from rules or habits in other fields of science. A recent practice at our university requests that new PhD's have to have at least three publications as first author in international journals in order to be eligible for a post-doc grant. Publications in conference proceedings are not accepted, even if they are refereed and published in international scientific journals! As a result, the PhDs from our field have great difficulties obtaining grants. Also, impact factors and the number of citations is becoming an increasingly important criterion for evaluation. Unfortunately, important deficiencies are present in the way these parameters are used. First of all, there are obvious mistakes in the list of journals belonging to a certain science domain as defined by ISI. For example, *Nuclear Physics B* is in the nuclear physics category while *Nuclear Instruments and Methods A* is not. Secondly, there is a tendency to merge nuclear physics and high-energy physics journals into one category. This has led to the following situation. A few years ago a study was performed where research groups from different European universities were compared on the basis of the average number of citations per publication normalized to the average citation score of the relevant science domain. The conclusion was that the top group in the domain of nuclear physics was from a university where no nuclear physics research was performed. After some investigation it turned out that this group was excellent in high-energy physics, publishing frequently in *Nuclear Physics B*. Another more recent example stems from an evaluation round whereby groups from different research fields were compared. The parameter used was the number of publications in the "top journals" of a particular field; "top journal" being defined as belonging to the top 10% of the journals with the highest impact factor. The evaluators decided to join particle and nuclear physics, which might seem reasonable as these fields are also discussed together at, for example, the funding agency. However, the publication practice in the particle physics community is vastly different from nuclear physics. The number of authors on a paper in particle physics is on

average about two orders of magnitude larger compared to papers in nuclear physics. This leads inevitably to different citation habits and different impact factors. As a consequence, the journals our community uses hardly appeared in the list of top journals and thus the nuclear physics groups received a low rating! It is interesting to note that even taking nuclear physics separately does not really make sense as, because of the small numbers involved, only one or two journals are included according to the "top journal" criterion. Needless to say, these evaluations can be devastating for the appreciation of our activities at the university and funding agency level. In the long term, it might reduce the spectrum of scientific journals of our field as groups are forced to publish only in the "top" journals. Our community has to be very attentive to these tendencies, investigate the way these measurable quantities are defined and used, and react in a coherent way.

However, we also have to critically assess our own practice of publishing workshop and conference proceedings. Every workshop and conference nowadays wants to have its own, eventually refereed, proceedings resulting in an over production. This also induces a lot of duplication, as the results will and should be presented in a regular journal. Note that the shelf half-life of proceeding is often very short. With the availability of the Internet it is much more rewarding to have the talks on the web, eventually in a shortened version, so that everybody can have access to the presentation right after the workshop or conference. In this way the interesting information is only a "mouse click away" and publishing real proceedings can thus be limited to the most important conferences; but *not* in regular journals. For many good reasons, like the limited number of pages for each contribution, the preliminary results presented, or the wild ideas put forward at conferences, the refereeing process for conference proceedings is less strict compared to refereeing of regular articles. Contributions to proceedings are on average hardly cited. As a consequence, publishing conference proceedings in refereed journals lowers the impact factor of the journals substantially and dilutes the quality of our regular papers. Some journals, for example, *Nuclear Physics B*, have already reacted to this by making a separately available journal for the conference proceedings.

Our community should start an active discussion on publication strategies in a coordinated way and on new ways to spread information presented at workshops and conferences. We have to investigate whether and how our common publication practice should be changed. Other aspects, which I did not touch upon but that should be considered as well, are the very high cost of certain journals and the new possibilities offered by the web. At the same time we should prepare for and adapt to the new evaluation criteria that are being used. It would be very helpful if international organizations (e.g, NuPECC and NSAC) take up a coordinating role in such discussions.

Let me end with the following illustrative anecdote that partly triggered the "to publish or not to publish in proceedings" question. At a workshop some time ago new measurements were presented that were in clear conflict with earlier data. A colleague, who was involved in the older experiments and tried to make the controversy less sharp, pointed out that the older results were only presented at a conference and published in the proceedings, not in a real journal. It turned out to be a refereed conference proceeding published in an international journal. Isn't it time to rethink all of this?

PIET VAN DUPPEN
University of Leuven

On the Discovery of Superheavy Elements

SIGURD HOFMANN, GOTTFRIED MÜNZENBERG, AND MATTHIAS SCHÄDEL

Gesellschaft für Schwerionenforschung (GSI), Planckstrasse 1, D-64221 Darmstadt, Germany

Present Status of Experiments

Remarkable progress was made in recent years in the field of Superheavy Element (SHE) research. Figure 1 gives an overview of isotopes presently (November 2004) known or under investigation at the upper end of the chart of nuclei. The isotopes are marked in different gray nuances indicating α decay, β^- decay, β^+ decay or electron capture, and spontaneous fission. Also given are the measured half-lives. Dots and circles mark Compound Nuclei (CN) formed in complete fusion reactions. From the CN the evaporation residues which are detected in the experiments emerge by evaporation of neutrons.

Three different classes of reactions are emphasized in Figure 1. One is based on targets of ^{208}Pb and ^{209}Bi and projectiles of the most neutron rich isotopes of the even elements from Ca to Sr (given in the first column on the right side). These reactions are weakly exothermic and are therefore often named *cold fusion* reactions. At excitation energies of 10 to 20 MeV only one neutron is emitted from the CN.

Cold fusion reactions were first successfully studied at the cyclotrons U300 and U400 in Dubna using beams of isotopes from Ar to Ge [1]. However, beyond seaborgium (Z = 106) those experiments were based on mechanical transport devices were not sensitive enough to identify new elements.

The sensitivity of experiments was significantly increased when recoil separators and the implantation of residues into position sensitive detectors were introduced [2,3]. The separation and detection system, known as SHIP is shown in Figure 2 in its improved version as presently in use at GSI [4]. The range of detectable half-lives was increased on the one hand down to microseconds due to a fast in-flight separation and on the other hand up to hours due to position and time correlation measurements of the decay of the implanted nuclei, both allowing for measuring long decay chains.

In a first series of experiments from 1981 to 1984 the elements bohrium, hassium, and meitnerium (Z = 107, 108, and 109) were synthesized using cold fusion reactions. The lowest cross-section measured was 16 pb from the synthesis of one atom of ^{266}Mt in a two-week experiment.

During the following years the sensitivity was increased to a detection level of one atom per week at a cross-section of 1 pb. This became possible by increasing the beam intensity by a factor of three and by increasing the efficiency of SHIP and of the detection system by another factor of three.

Using the improved set-up, excitation functions of elements up to hassium were measured with high accuracy. The experiments showed that cross-section peaks are shifted to lower excitation energies with increasing element number. Based on this knowledge, proper beam energies were chosen for the synthesis of the new elements 110 to 112. The nuclei ^{269}110, ^{271}110, ^{272}111, and ^{277}112 were synthesized by detection of 3, 9, 3, and 1 α-decay chain, respectively. The decay chains are marked in Figure 1 by sequences of arrows. Cross-sections of 2.6, 15, 3.5, and 0.5 pb were measured. The experiments took place in the years 1994 and 1996. They lasted between 2 and 3 weeks each and an average beam dose collected was 1.2×10^{18} particles per week.

Element 110 was officially named darmstadtium (Ds) at GSI on December 2nd, 2003, after acceptance of the proposed name by the General Assembly of IUPAC in Ottawa, August 16, 2003. Synthesis and decay of ^{271}Ds was confirmed at GSI itself and also in recent experiments at RIKEN [5] and LBNL [6].

Three more decay chains of ^{272}111 were measured in 2000 at SHIP [7]. The previously measured decay data were confirmed and improved. The reaction ^{64}Ni + ^{209}Bi was also studied at RIKEN resulting in independent confirmation of our data [8]. We proposed the name roentgenium, symbol Rg, for element 111. IUPAC adopted our suggestion in a recent recommendation [9].

In the case of element 112 one more decay chain was measured in an experiment in 2000 [7]. Agreement with the data measured from the first decay chain was obtained for the first four α decays. However, different from the first chain, spontaneous fission was measured for ^{261}Rf instead of α decay. Such a spontaneous fission branching of ^{261}Rf was confirmed in a recent chemistry experiment. There, ^{269}Hs, the granddaughter of ^{277}112 was produced

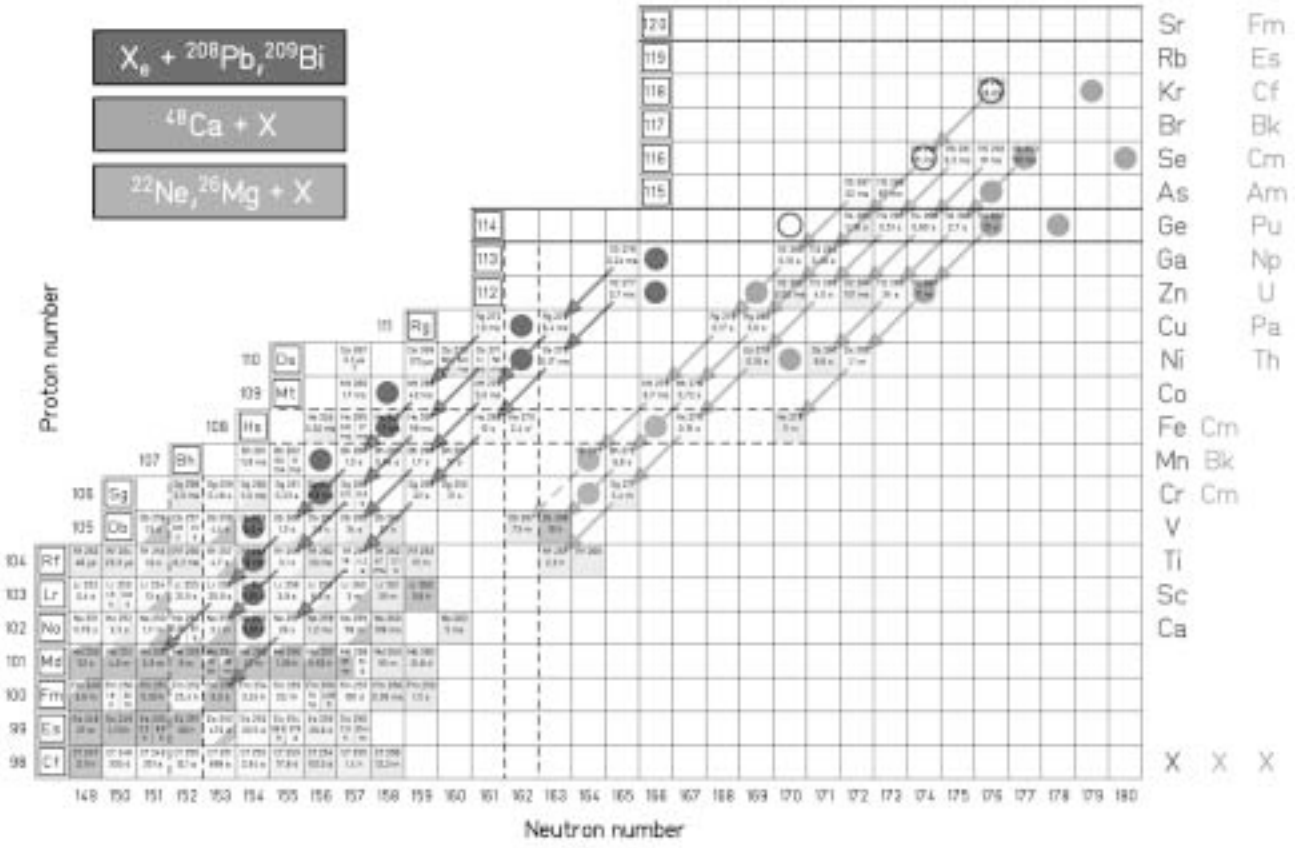

Figure 1. *Presently known nuclei with N ≥ 149 and Z ≥ 98. See text for an explanation of the symbols.*

in the reaction $^{26}Mg + ^{248}Cm \rightarrow ^{274}Hs^*$, and after chemical separation of hassium from other reaction products the decay chain was studied by means of silicon detectors [9]. A direct confirmation of both the cross-sectioned and the decay properties of $^{277}112$ was obtained in an experiment at RIKEN in April–May 2004 [11]. Using the same reaction as in the GSI experiment, $^{70}Zn + ^{208}Pb \rightarrow ^{278}112^*$, two decay chains were measured. Both ended by spontaneous fission of ^{261}Rf.

A world record concerning measurement of low cross-sections was established in the periods from September–December 2003 and July–August 2004 at RIKEN [12]. During a 140 day experiment, 79 days with beam on target, one decay chain was observed in the reaction $^{70}Zn + ^{209}Bi \rightarrow ^{279}113^*$. It was assigned to the new isotope $^{278}113$. The chain is connected to the known nuclei ^{266}Bh and ^{262}Db, where it ends by fission. By the first two α decays the new isotopes ^{274}Rg and ^{270}Mt were produced. The measured cross-section was 55^{+150}_{-45} fb. This value is in agreement with the cross-section systematic as discussed in the following.

The circles in Figure 1 mark CN of reactions with beams of ^{76}Ge, ^{82}Se, and ^{86}Kr and targets of ^{208}Pb, which were investigated in recent years at GANIL (114, 118), GSI (Z = 116, 118), LBNL (118), and RIKEN (118) without any positive result. Cross-section limits reached values of about 0.5 to 1 pb.

The second class of reactions emphasized in Figure 1 was started to be studied at the U400 in Dubna by FLNR-LLNL and FLNR-GSI collaborations. These reactions, which are being investigated systematically since 1998, are based on an intensive beam of ^{48}Ca ions and targets of ^{232}Th, ^{238}U, $^{242,244}Pu$, ^{243}Am, $^{245,248}Cm$, and ^{249}Cf [11,12]. The evaporation residues are separated from the beam by using either the Dubna gas-filled separator DGFRS or the energy filter VASSILISSA.

CN of reactions investigated at Dubna are also shown in Figure 1.

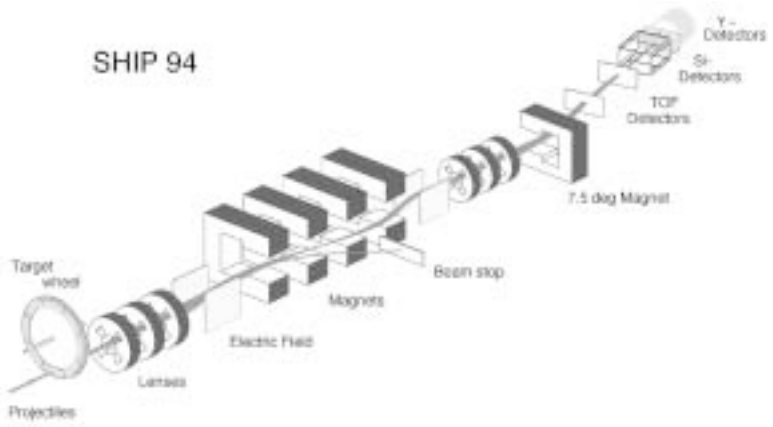

Figure 2. *The velocity filter SHIP (Separator for Heavy Ion reaction Products) and its detection system. For details of the set-up see Ref. [2–4].*

Reactions based on actinide targets are more exothermic than cold fusion reactions and are therefore often named *hot fusion reactions*. At excitation energies of 35 to 50 MeV a number of 3 to 5 neutrons is emitted. The measured decay chains of the evaporation residues and their assignment are given in Figure 1.

For these reactions the correct number of emitted neutrons is difficult to determine from single decay chains, because the new nuclei are located in a completely new area of the chart of nuclei. Different from the GSI data the Dubna decay chains are not connected to known nuclei. Therefore additional measurements, as, for example, direct mass measurements or element identification by chemical means are needed for establishing an unambiguous assignment.

Another method that was actually used at Dubna in the most recent experiments [12] is the systematic study of cross bombardments and measurement of excitation functions. From a total of seven reactions investigated and a total of 39 decay chains measured, a consistent assignment results, which is given in Figure 1, and which was presented in most recent publications [11,12].

The most significant results of the Dubna experiments, which are discussed in more detail in subsequent sections, are first, the increase of half-life of the new isotopes with increasing neutron number and second, the relatively high cross-sections that scatter around 1 pb even up to the synthesis of element Z = 118.

The third class of reactions is also based on hot fusion reactions. With beams of ^{22}Ne and ^{26}Mg and targets of ^{248}Cm and ^{249}Bk very neutron rich CN of Sg, Bh, and Hs are produced. After

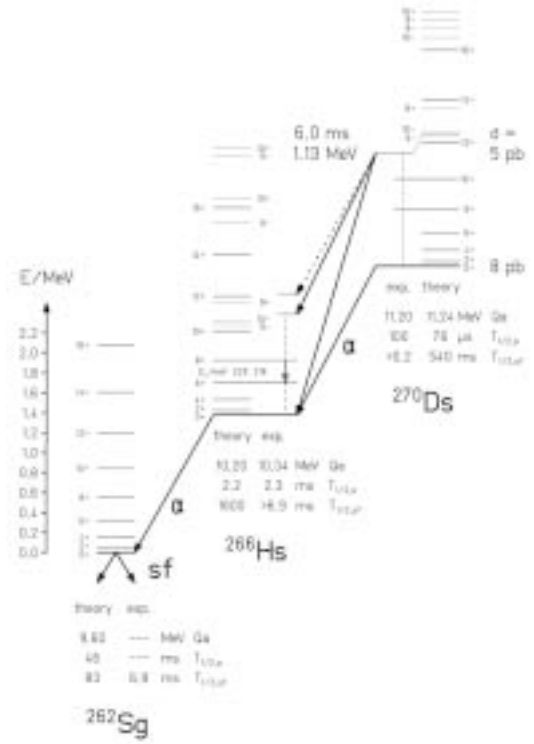

Figure 3. *Assignment of measured α and γ decay data and spontaneous fission observed in the reaction ^{64}Ni + ^{207}Pb → ^{271}Ds*. The data were assigned to the ground-state decays of the new isotopes ^{270}Ds, ^{266}Hs, and ^{262}Sg and to a high spin K isomer in ^{270}Ds. Arrows in bold represent measured α and γ rays and spontaneous fission. The proposed partial level schemes are taken from theoretical studies of rotational levels [19], of K isomers [20], and of α energies and spontaneous fission half-lives [21,22]. For a detailed discussion see Ref. [18].*

evaporation of 4 or 5 neutrons isotopes emerge with half-lives long enough (>1 s) in order to study these elements by chemical means. The case of ^{269}Hs was already mentioned before.

After the recent Dubna experiments revealed long half-lives (see Figure 1) and reasonable yields for the synthesis of elements based on reactions with ^{48}Ca, experiments are under way to study the chemical properties of element 112 and beyond. First results on element 112 were already obtained; however, these data are waiting to be confirmed in upcoming experiments. A review on chemical studies is given in Ref. [13].

Another two classes of heavy element experiments are dealing with *in-beam spectroscopy* and *focal-plane spectroscopy*. Isotopes of nobelium to seaborgium are produced with cross-sections of 3 μb to 3 nb, respectively, using cold fusion reactions. The yields are sufficiently high to measure γ rays or conversion electrons emitted from nuclei during or just after the reaction with appropriate detectors installed at the target area. Individual nuclei are identified by means of the Recoil Decay Tagging method (RDT), a delayed coincidence technique between radiation emitted at the target, implantation of the evaporation residue into the detector behind the separator and its radioactive decay [14]. Examples are the studies of nobelium isotopes [15,16].

Focal plane spectroscopy exploits the relatively high yield of heavy nuclei at highest beam intensities produced at cross-sections down to values of only a few tenths of nanobarns. The decay of ground-states and isomeric states, α-decay fine structure, β decay, and spontaneous fission is studied in a environment of low background behind the separator. Coincidences with conversion electrons or γ rays supplement the measurements.

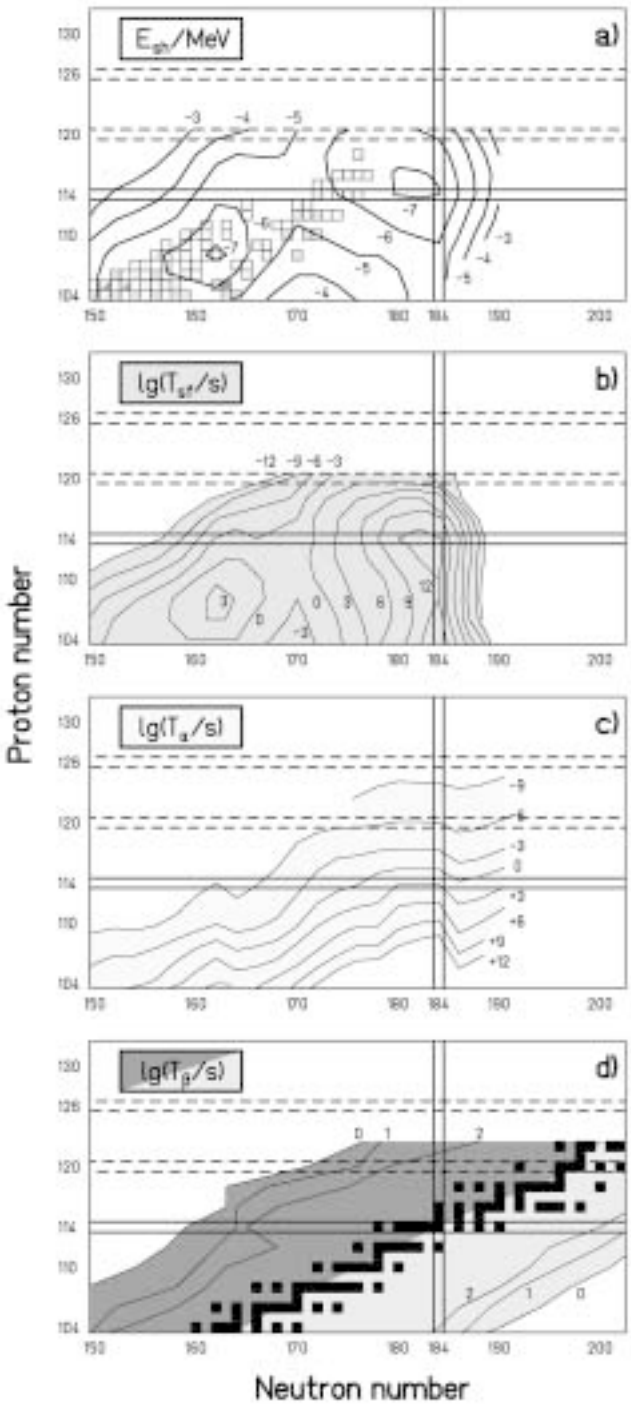

Figure 4. *Shell-correction energy (a) and partial spontaneous fission, α and β half-lives (b–d). The calculated values in (a)–(c) are taken from Ref. [22,23] and in (d) from Ref. [26]. The squares in (a) mark the nuclei presently known or under investigation, the filled squares in (d) mark the β stable nuclei.*

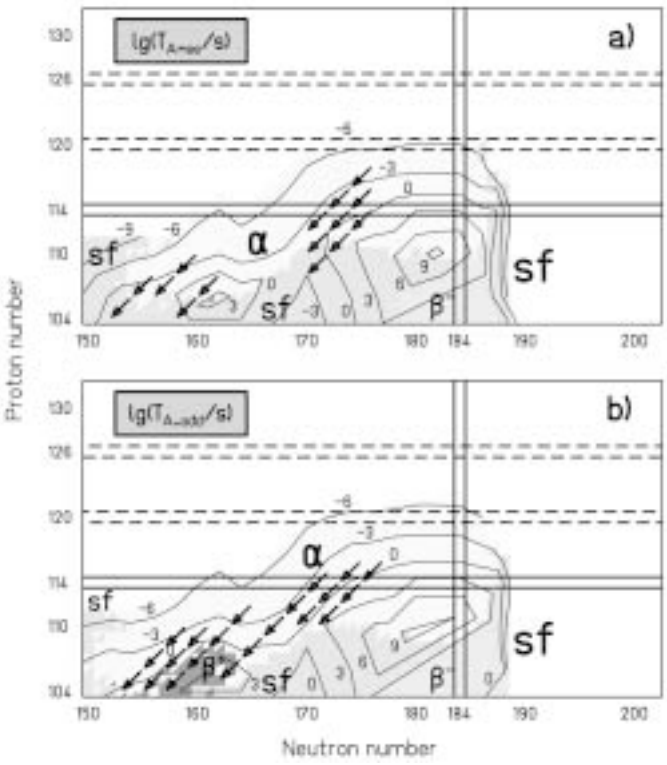

Figure 5. *Dominating α, β, and spontaneous fission half-lives: (a) for even-even nuclei; (b) for odd-A nuclei. The decay chains of nuclei presently known or under investigation are also given.*

Examples are given in Ref. [17].

An extraordinary case is shown in Figure 3. It demonstrates that even on a cross-section level of a few picobarns spectroscopic information can be obtained from only a few number of nuclei produced [18].

Nuclear Structure and Decay Properties of SHE

Knowledge of the ground-state binding energy provides the basic step to determine the stability of SHEs. In macroscopic-microscopic models the binding energy is calculated as the sum of a predominating macroscopic part (derived from the liquid-drop model of the atomic nucleus) and a microscopic part (shell correction energy derived from the nuclear shell model). The shell correction energy is plotted in Figure 4a using data from Ref. [23]. Two equally deep minima are obtained, one at Z = 108 and N = 162 for deformed nuclei with deformation parameters $\beta_2 \approx 0.22$, $\beta_4 \approx -0.07$ and the other one at Z = 114 and N = 184 for spherical SHEs. Different results are obtained from self-consistent Hartree-Fock-Bogoliubov calculations and relativistic mean-field models [24,25]. They predict for spherical nuclei shells at Z = 114, 120 or 126 (indicated as dashed lines in Figures 4 to 6) and N = 184 or 172, with shell strengths being also a function of the number of neutrons and protons, respectively.

The knowledge of ground-state binding energies, however, is not sufficient for the calculation of partial spontaneous fission half-lives. Here it is necessary to determine the size of the fission barrier over a wide range of deformation. The most accurate data were obtained for even-even nuclei using a macroscopic-microscopic model [22]. Partial spontaneous fission half-lives are plotted in Figure 4b.

Partial α half-lives decrease almost monotonically from 10^{12} s down to 10^{-9} s near Z = 126 (Figure 4c). The valley of β-stable nuclei passes through Z = 114, N = 184. At a distance of about 20 neutrons away from the bottom of this valley, β half-lives of isotopes have dropped down to values of one second [26] (Figure 4d).

Combining results from the individual decay modes one obtains the dominating partial half-life as shown in Figure 5a,b for even-even and odd A nuclei. The two regions of deformed heavy nuclei near N = 162 and spherical SHEs merge and form a region of α emitters surrounded by spontaneously fissioning nuclei. The longest half-lives are 1000 s for deformed heavy nuclei and 30 y for spherical SHEs.

Also drawn in the figure are the measured decay chains and their assignment to isotopes of the elements from hassium to 118. Taking into account the uncertainties related with the calculated partial half-lives, we find generally good agreement with the experimental data. Especially the termination of the decay chains by spontaneous fission is well reproduced.

The interesting question arises, if and to which extent uncertainties related to the location of proton and neutron shell closures will change the half-lives of SHEs. Partial α and β half-lives are only insignificantly modified by shell effects, because their decay process occurs between neighboring nuclei. This is

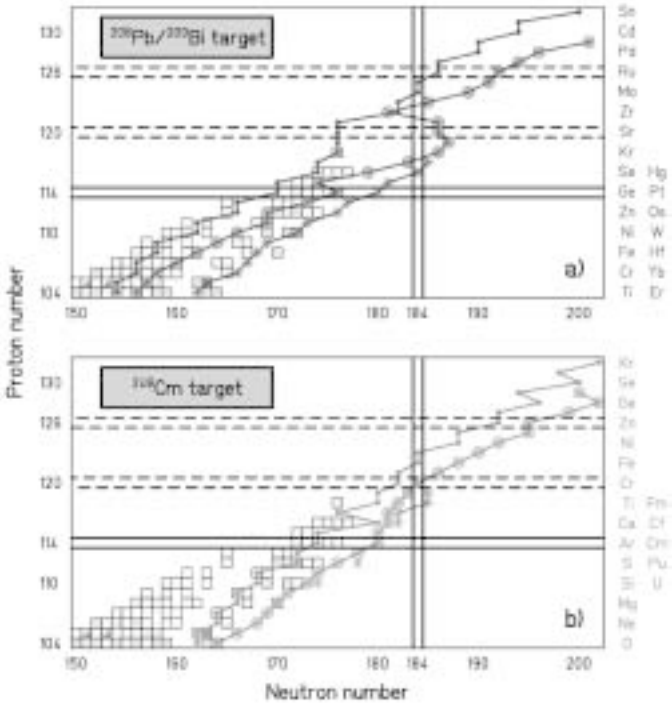

Figure 6. *Most neutron rich CN produced in reactions using stable and radioactive beams and targets. In Figure 6a the curve marked with dots (•) shows the most neutron rich CN that can be produced with ^{208}Pb or ^{209}Bi targets and beams of the most neutron rich stable isotopes of the elements from Ti to Sn, given in the first column at the right ordinate. On the average the accessible region is extended by 4 to 5 neutrons to the right using radioactive isotopes of these elements (symbol ⊗ in a). As possible most neutron rich radioactive projectiles those isotopes were taken into account that could be produced with intensities of at least 10^9 /s according to the data presented in the RIA proposal [27]. Striking is the wide extension of possible CN to the neutron rich side at Z = 120 using beams of Kr, Rb, and Sr. The reason is that these nuclei are available as fission fragments and can be extracted from ion sources with high yield, too. More neutron rich nuclei of elements below Z = 118 can be produced using the radioactive beams of ^{96}Kr or ^{98}Rb and targets of stable neutron rich isotopes of elements below Pb from Hg down to Er (second column on the right ordinate, curve marked with symbol *). In the lower plot, b, the equivalent combinations are given for reactions using a ^{248}Cm target and stable and radioactive beams.*

different for fission half-lives of SHEs, which are primarily determined by shell effects. However, the uncertainty related to the location of nuclei with the strongest shell-effects, and thus longest partial fission half-life at Z = 114, 120 or 126 and N = 172 or 184, is irrelevant concerning the longest 'total' half-life of SHEs. All regions for these SHEs are dominated by α decay. Alpha-decay half-lives will only be modified by a factor of up to approximately 100, if the double shell closure is not located at Z = 114 and N = 184.

The line of reasoning is, however, different concerning the production cross-section. The survival probability of the CN is determined among other factors significantly by the fission-barrier. Therefore, with respect to an efficient production yield, the knowledge of the location of minimal negative shell-correction energy is highly important. However, it may also turn out that shell effects in the region of SHEs are distributed across a number of subshell closures. In that case a wider region of less deep shell-correction energy would exist with corresponding modification of stability and production yield of SHEs.

Compound Nuclei with Radioactive Beams

CN that could be produced concerning the availability of beams and targets are plotted in Figure 6. The graphs demonstrate the extension into the region of SHEs which may become possible with radioactive beams assuming that sufficient beam intensities will become available. The nuclei presently known or under investigation are marked by squares.

Cross-Sections, Fusion Valleys, and Excitation Energy

The main features that determine the fusion process of heavy ions are (1) the fusion barrier and the related beam energy and excitation energy, (2) the ratio of surface tension versus Coulomb repulsion, that determines the fusion probability and which strongly depends on the asymmetry of the reaction partners (the product Z_1Z_2 at fixed $Z_1 + Z_2$), (3) the impact parameter (centrality of collision) and related angular momentum, and (4) the competition of neutron evaporation and of γ emission versus fission of the CN.

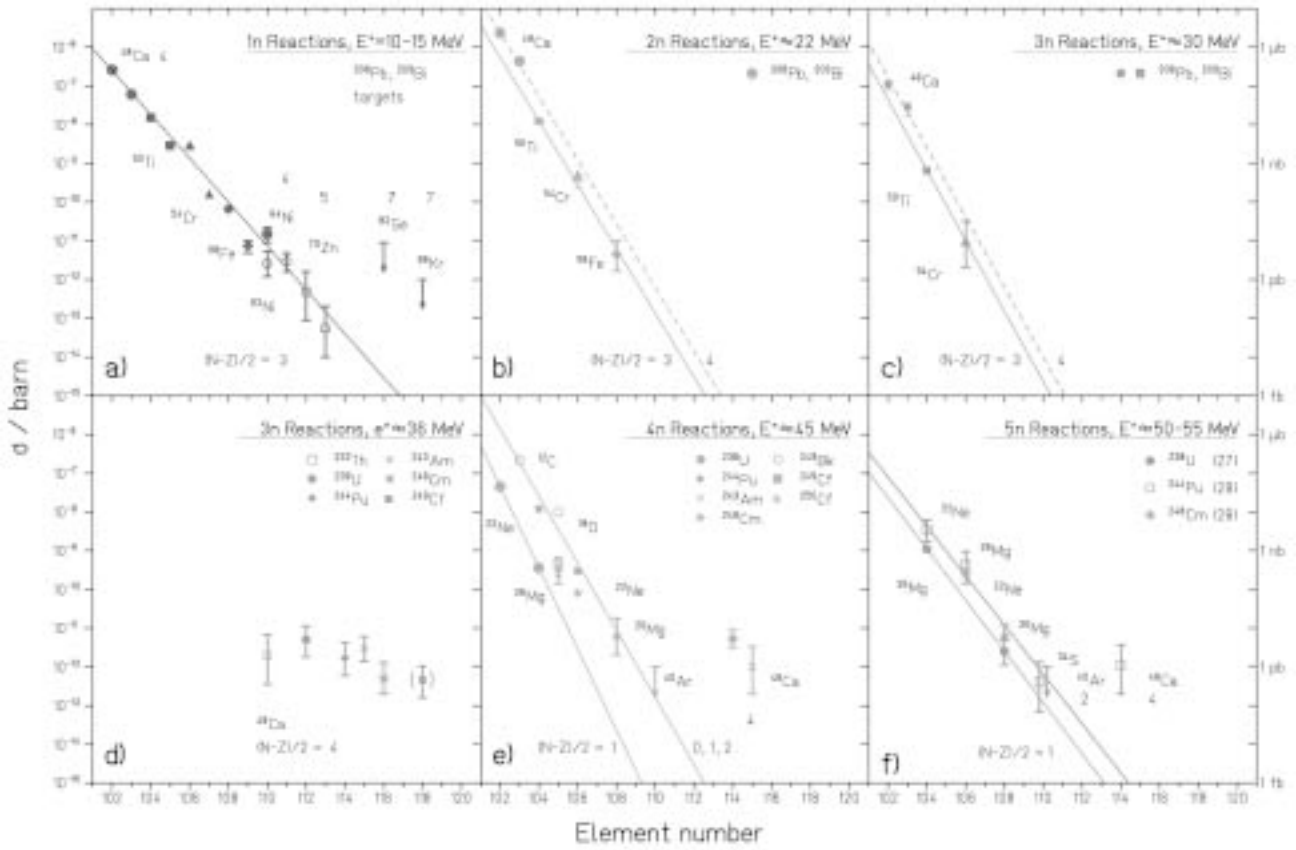

Figure 7. *Measured cross-sections and cross-section limits.*

Coulomb repulsion starts to act severely in the case of cold fusion reactions when producing elements beyond fermium. From there on a continuous decrease of cross-section was measured from microbarns for the synthesis of nobelium down to picobarns for the synthesis of element 112. The measured data are shown in Figure 7a–c.

In the case of hot fusion reactions the trend given by the experimental data is different, as shown in Figure 7d–f. Here, fission competition in the deexcitation process may govern the decrease. Surprising, however, using a ^{48}Ca beam and actinide targets, the cross-sections of 3n, 4n, and 5n evaporation channels of elements beyond Z = 110 stay rather constant at a level of about 0.5 to 5 pb.

A number of excitation functions was measured for the synthesis of elements from nobelium to darmstadtium in cold fusion reactions. The curves are shown together with the two data points for ^{277}112 in Figure 8. Maximum evaporation residue cross-sections (1n channel) were measured at beam energies well below a contact configuration, where projectile and target nucleus come to rest in the center of the mass system according to the Bass model [28].

For the hot fusion reaction ^{48}Ca + ^{244}Pu → ^{292}114* the excitation function of the 4n channel was measured recently at Dubna [12], see lowest panel in Figure 8. Here the peak is located well above the contact configuration calculated from a mean value of the Coulomb potential of the deformed target nucleus. This shift as well as the increased width of the curve (10.6 MeV instead of 4.6 MeV FWHM for ^{266}Hs) are in accord with an orientation effect on fusion using a deformed target nucleus. The shift to higher energy indicates collisions in direction of the short deformation axis.

It was pointed out in the literature [29] that closed shell projectile and target nuclei are favorable synthesizing SHEs. The reason is not only a low

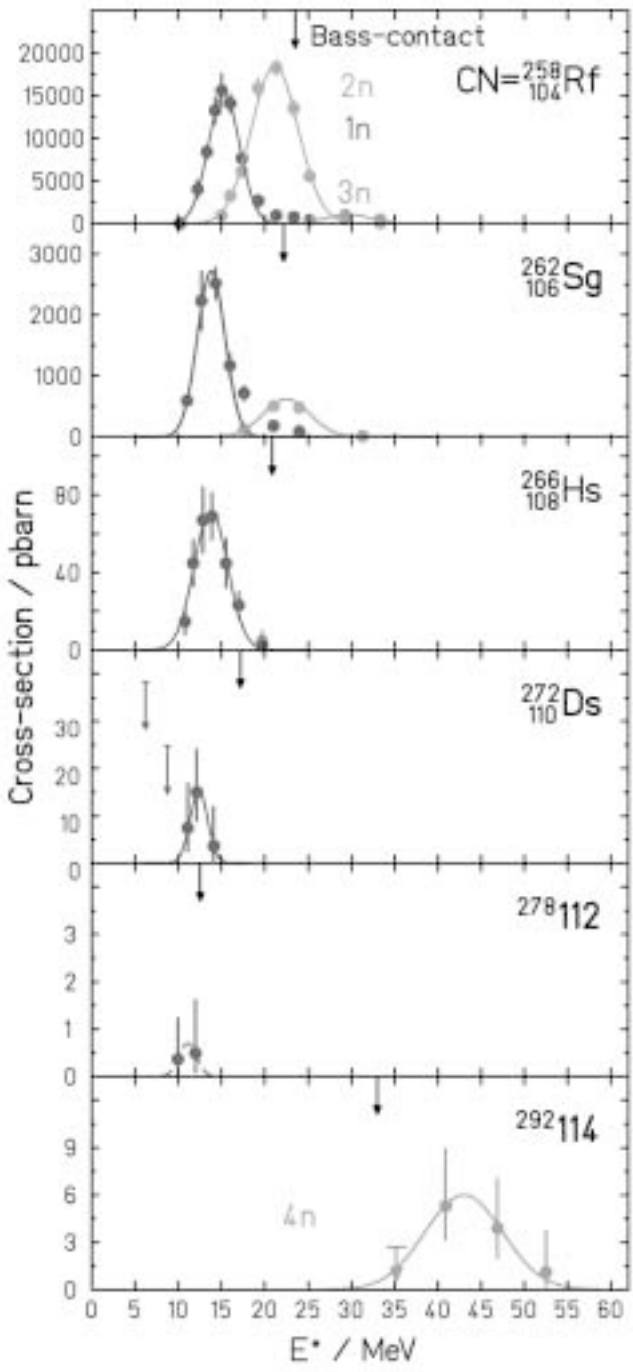

Figure 8. *Measured excitation functions.*

(negative) reaction Q-value and thus a low excitation energy, but also that fusion of such systems is connected with a minimum of energy dissipation. The fusion path proceeds along cold fusion valleys, where the reaction partners maintain kinetic energy up to the closest possible distance. In this view the difference between cold and hot fusion is not only a result from gradually different values of excitation energy, but there exists a qualitative difference, which is on the one hand (cold fusion) based on a well ordered fusion process along paths of minimum dissipation of energy, and on the other hand (hot fusion) based on a process governed by the formation of a more or less energy equilibrated CN. The use of the double magic ^{48}Ca and actinide targets seems to proceed via an intermediate fusion process, possibly along a fusion valley less pronounced than in the case of cold fusion. Triggered by the recent experimental success of heavy element synthesis, a number of theoretical studies are in progress aiming to obtain a detailed understanding of the processes involved [30–37].

Summary and Outlook

The experimental work of the last two decades has shown that cross-sections for the synthesis of the heaviest elements decrease almost continuously. However, recent data on the synthesis of elements 112 to 116 at Dubna using hot fusion seem to break this trend when the region of spherical SHEs is reached. Therefore a confirmation is urgently needed that the exploration of the "island" has finally started and can be performed and continued even on a relatively high cross-section level.

However, the progress toward the exploration of the island of spherical SHEs is difficult to predict. Despite the exciting new results, many questions of more general character are still awaiting an answer. New developments will not only make it possible to perform experiments aimed at synthesizing new elements in reasonable measuring times, but will also allow for a number

of various other investigations covering reaction physics and spectroscopy.

One can hope that, during the coming years, more data will be measured in order to promote a better understanding of the stability of the heaviest elements and the processes that lead to fusion. A microscopic description of the fusion process will be needed for an effective explanation of all measured phenomena in the case of low dissipative energies. Then, the relationships between fusion probability and stability of the fusion products may also become apparent.

An opportunity for the continuation of experiments in the region of SHEs at decreasing cross-sections afford, among others, further accelerator developments. High current beams and radioactive beams are options for the future. At increased beam currents, values of tens of particle μA's may become accessible, the cross-section level for the performance of experiments can be shifted down into the region of tens of femtobarns, and excitation functions can be measured on the level of tenths of picobarns. High currents, in turn, call for the development of new targets and separator improvements. Radioactive ion beams, not as intense as the ones with stable isotopes, may allow for approaching the closed neutron shell N = 184 already at lighter elements. The study of the fusion process using radioactive neutron-rich beams is of highest interest.

The half-lives of spherical SHEs are expected to be relatively long. Based on nuclear models, half-life values from microseconds to years have been calculated for various isotopes in the region of the heaviest elements.

This wide range of half-lives encourages the application of a wide variety of experimental methods in the investigation of SHEs, from the safe identification of short lived isotopes by recoil-separation techniques to atomic physics experiments on trapped ions. Long-lived isotopes allow for the study of relativistic effects on the chemical properties of SHEs and atomic number identification by chemical methods.

References

1. Yu. Ts. Oganessian et al., *Nucl. Phys.* A239 (1975) 157.
2. G. Münzenberg et al., *Nucl. Instr. Meth.* 161 (1979) 65.
3. S. Hofmann et al., *Z. Phys.* A291 (1979) 53.
4. S. Hofmann and G. Münzenberg, *Rev. Mod. Phys.* 72 (2000) 733.
5. K. Morita et al., *Eur. Phys. J.* A21 (2004) 257.
6. T.N. Ginter et al., *Phys. Rev.* C67 (2003) 064609.
7. S. Hofmann et al., *Eur. Phys. J.* A14 (2002) 147.
8. K. Morita et al., *J. Phys. Soc. Jpn.* 73 (2004) 1738.
9. www.iupac.org/news/archives/2004/naming111.html (2004).
10. Ch. E. Düllmann et al., *Nature* 418 (2002) 859.
11. K. Morita, et al., Proceedings International Symposium on Exotic Nuclei, Peterhof, Russia, July 5–12 (2004), to be published.
12. K. Morita et al., *J. Phys. Soc. Jpn.* 73 (2004) 2593.
13. Yu. Ts. Oganessian et al., *Phys. Rev.* C69 (2004) 021601.
14. Yu. Ts. Oganessian et al., *Phys. Rev.* C69 (2004) 054607.
15. M. Schädel, Ed., The Chemistry of Superheavy Elements, Kluwer Academic Publisher, Dordrecht (2003), pp. 318.
16. R.-D. Herzberg et al., *Phys. Rev.* C65 (2001) 014303.
17. F.P. Heßberger et al., *Eur. Phys. J.* A12 (2001) 57.
18. S. Hofmann et al., *Eur. Phys. J.* A10 (2001) 5.
19. I. Muntian et al., *Phys. Rev.* C60 (1999) 041302.
20. S. Cwiok et al., *Phys. Rev. Lett.* 83 (1999) 1108.
21. R. Smolanczuk, *Phys. Rev. Lett.* 83 (1999) 4705.
22. R. Smolanczuk et al., *Phys. Rev.* C52 (1995) 1871.
23. R. Smolanczuk and A. Sobiczewski, Proceedings XV. Nuclear Physics Divisional Conference on Low Energy Nuclear Dynamics, World Scientific, Singapore (1995), p. 313.
24. S. Cwiok et al., *Nucl. Phys.* A611 (1996) 211.
25. M. Bender et al., *Phys. Lett.* B515 (2001) 42.
26. P. Möller et al., *Atomic Data and Nucl. Data Tables* 66 (1997) 131.
27. RIA, The Rare sotope Accelerator Project, www.phy.anl.gov/ria (2000).
28. R. Bass, *Nucl. Phys.* A231 (1974) 45.
29. R.K. Gupta et al., *Z. Phys.* A283 (1977) 217.
30. V.Yu. Denisov and S. Hofmann, *Phys. Rev.* C61 (2000) 034606.
31. V.Yu. Denisov and W. Nörenberg, *Eur. Phys. J.* A15 (2002) 375.
32. Y. Aritomo et al., *Phys. Rev.* C59 (1999) 796.
33. V.I. Zagrebaev, *Phys. Rev.* C64 (2001) 034606.
34. G. Giardina et al., *Eur. Phys. J.* A8 (2000) 205.
35. R. Smolanczuk, *Phys. Rev.* C63 (2001) 044607.
36. G.G. Adamian et al., *Phys. Rev.* C69 (2004) 011601, 014607, 044601.
37. W.J. Swiatecki et al., *Int. J. Mod. Phys.*, E13 (2004) 261.

Superheavy Element Chemistry

ANDREAS TÜRLER AND A. B. YAKUSHEV

Institut für Radiochemie, Technische Universität München, Walther-Meissner-Strasse 3
D-85748 Garching, Germany

Status and Perspectives

The discovery of new elements and their correct placement in the Periodic Table has originally been the domain of chemists. Indeed, the discovery of new elements up to mendelevium (Md, $Z = 101$) was accomplished by chemical means [1]. The decreasing production cross sections, that nowadays are of the order of one picobarn or even less for the heaviest known nuclei, and the rapidly diminishing half-lives made manual chemical investigations of elements beyond $Z = 105$ virtually impossible. Thus, the synthesis and identification of new elements has completely shifted to nuclear physics and led to the discovery of more than ten new elements. However, the placement of a new element in the Periodic Table is not only based on its proton number but also on its chemical properties, which are determined by its electronic structure. Relativity that is important in determining the nuclear shell structure and thus the decay properties of superheavy elements (SHE), is extremely important in defining the chemical properties. Therefore, not only the physics but also the chemistry of SHE is extremely interesting and rewarding to be studied. With $Z = 104$, Rf, starts a new series of d-elements, the so-called transactinides (see Figure 1). Because the liquid drop fission

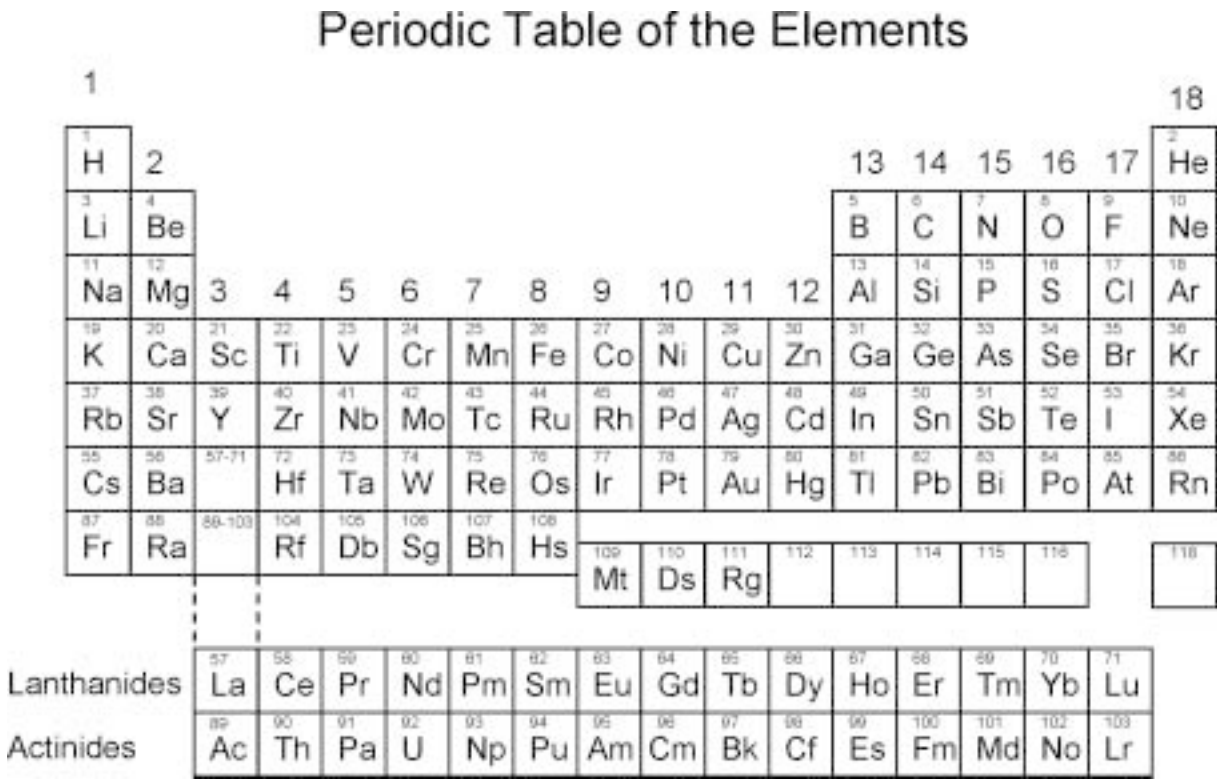

Figure 1. *Periodic Table of the elements including recently reported discoveries. See text for detailed explanations.*

barrier also disappears around $Z = 104$ the term SHE is often used as a synonym for transactinide elements.

Despite the numerous difficulties involved in chemically isolating one single, relatively short-lived atom from a plethora of unwanted by-products of the nuclear production reaction, remarkable progress was made in recent years. This progress can be attributed to the discovery of enhanced nuclear stability close to the vicinity of the previously predicted deformed shells at $Z = 108$ and $N = 162$ [2], which provided chemists with sufficiently long-lived isotopes of seaborgium (Sg, $Z = 106$) [3], bohrium (Bh, $Z = 107$) [4] and even hassium (Hs, $Z = 108$) [5]. By developing fast, automated, and sensitive techniques chemists have discovered or significantly contributed to the characterization of the new nuclides ^{265,266}Sg [6], ^{266,267}Bh [7] and ^{269,270}Hs [8]. As in experiments of our nuclear physics colleagues, the production of a heavy nucleus was detected by registering its nuclear decay, which for many super-heavy nuclei consists of unique alpha-particle decay chains quite often terminated by spontaneous fission. The knowledge and understanding of the chemistry of SHE, especially of the early transactinides Rf, Db, and Sg and their compounds, both experimentally and theoretically, is nowadays quite extensive as documented by the first textbook entitled "The Chemistry of Superheavy Elements" edited by M. Schädel [9]. Although rapid chemical separations in aqueous solution were (and are) the method of choice for detailed investigations of Rf and Db [10,11], the development of gas-phase chemical separation methods have allowed first chemical studies of all transactinide elements up to Hs [12–14]. The discovery of longer-lived (half-lives of several seconds) isotopes of elements 110 through 114 in ^{48}Ca-induced reactions on actinide targets at the Flerov Laboratory of Nuclear Reactions in Dubna has opened fascinating new perspectives to experimentally study the chemistry of even the heaviest elements in the Periodic Table [15]. Currently, experiments are conducted to elucidate the chemical properties of element 112 (E112) [16–18] and also element 114 (E114) in their elemental state. There are already indications that E112 behaves chemically not at all similarly to its lighter homolog Hg. Because all of the decay chains of the newly discovered neutron-rich nuclides end in an uncharted area of the chart of nuclides a chemical identification of one of the members of these decay chains could clearly pinpoint the atomic number of the newly synthesized elements. Therefore, a chemical separator system can be regarded as a somewhat slow, but efficient Z-separator. Because chemical separator systems are nearly independent on the production reaction, thick targets and very asymmetric reactions can be employed to access neutron-rich heavy nuclei.

Figure 1 displays a modern Periodic Table of the elements. Elements whose chemical behavior has not yet been experimentally investigated are shown below their expected positions. The element names are those accepted, or in the case of element 111 (roentgenium, Rg), recommended by IUPAC. Provisional names such as ununbium (Uub, $Z = 112$) are not indicated.

In the following the expected chemical properties of Hs and heavier elements, the available chemical separation techniques, and the latest results of recent chemistry experiments are presented.

Chemical Properties of SHE and their Compounds

Studies of transactinide elements by chemical means rely strongly on predictions of their chemical properties. In order to plan a separation scheme, the stability of compounds and their physicochemical properties have to be judged on the basis of predictions. Traditionally, the chemical properties of an unknown element and its compounds were predicted by exploiting the fundamental relationships of the physicochemical data of the elements and their compounds within the groups and the periods of the Periodic Table. Because relativistic effects are increasing proportionally with Z^2, extrapolations of chemical properties from lighter homolog elements must fail at some point. Here, the only alternative are fully relativistic calculations. Generally, three relativistic effects are observed. First, due to the high probability density near the highly charged nucleus the $s_{1/2}$ and $p_{1/2}$ orbital radii are contracting and the binding energies are increasing. These are called "direct" relativistic effects [19]. Second, the spin-orbit splitting produces two levels for each ℓ quantum number. Third, due to the increased screening of the nuclear charge by the $s_{1/2}$ and $p_{1/2}$ orbitals the d and f orbitals are expanding spatially and are energetically destabilized. This was named an "indirect" relativistic effect [19], but this effect directly influences the outermost electrons that are largely responsible for the chemical behavior of an atom. At present it is not possible to directly compute physicochemical properties of a molecule. All-electron calculations of molecules containing transactinide elements are exceedingly difficult due to the large number of electrons involved. Nonetheless, also due to the

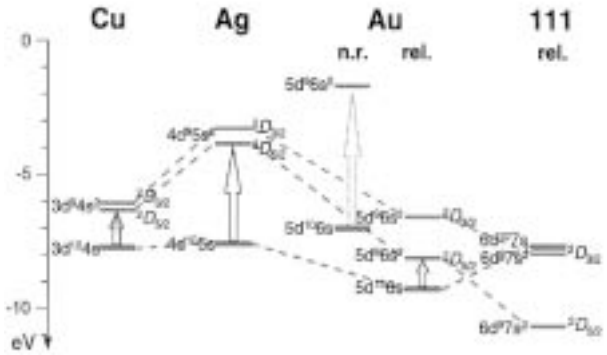

Figure 2. *Energy levels of group 11 elements Cu, Ag, Au, and E111 (Rg). In the case of Au also the calculated non-relativistic energy level scheme is shown. The calculated relativistic energy levels for E111 are taken from Ref. [23].*

enormously increasing computing power, theoretical calculations have progressed now to the point that a number of relevant atomic and molecular properties can be computed. This article will focus on some aspects of the expected chemical properties of elements with $Z \geq 108$. Comprehensive reviews on the calculated chemical properties of the early transactinides can be found in the literature [20,21].

Sometimes Mother Nature is rather kind to chemists and provides them with favorable, very clear cut cases. Such a case constitutes the chemistry of Hs. If Hs has any resemblance to its lighter homolog element Os then it should also form molecules of the type MO_4 (M = Os, Hs). Due to the perfect tetrahedral symmetry of OsO_4, this compound is very volatile, and only interacts very weakly with non-reducing surfaces, similar to a noble gas. Relativistic molecular orbital calculations by Pershina et al. [22] confirmed that indeed HsO_4 must be a very stable molecule and that its volatility should be very similar to its lighter homolog compound OsO_4. This exceptional chemical property distinguishes Os and Hs from other d-elements and allows a clear assignment to group 8 of the Periodic Table. Thus, experimentalists successfully took on the daunting task to build a separator system that allowed the isolation of Hs as volatile HsO_4.

An illustrative example of the increasing influence of relativistic effects is shown in the case of the so-called coinage metals Cu, Ag, Au and Rg (Z = 111). In Figure 2, the ground state electronic configuration and the first exited states of Cu, Ag, Au and Rg [23] are shown. For Au also the hypothetical non-relativistic case has been calculated. Cu, Ag, and Au all have the same $d^{10}s$ ground state configuration. As can be clearly seen, the spin-orbit splitting of the d^9s^2 first exited state is increasing with the proton number. A possible reason for the red color of Cu and the colorless appearance of Ag lies in the substantially higher first exited state of Ag, which leads to an absorption that lies in the ultraviolet region. If this trend would continue, Au should be a colorless metal that is less noble than Cu and Ag due to the lower ionization energy. However, the relativistic stabilization of the s orbitals and the increasing spin-orbit splitting make Au a yellow metal with a more noble character than Cu or Ag. The strong relativistic stabilization of the filled s^2-orbital and the further increased spin-orbit splitting lead to an inversion of states in Rg. Thus, Rg is expected to have a $6d^97s^2$ ground state; the higher ionization energy compared to Au (≈10.6 eV vs. 9.21 eV) and the lower electron affinity (≈1.55 eV vs. 2.31 eV) will probably make Rg an even nobler metal. The trends observed in group 11 are also persisting in groups 12 through 14.

Another chemically very favorable case constitutes E112 as an expected homolog of Hg. E112 is expected to have an ionization potential which is more than 1.5 eV higher than that of Hg. Similar to Hg, E112 should not have a bound anion. Therefore, E112 is expected to be rather inert in its elemental state. It is well known that Hg is a very volatile element, but it interacts strongly with other metals such as Zn or Au to form amalgams. Yakushev et al. demonstrated that single atoms of Hg can quantitatively be adsorbed on an Au surface from a stream of He [16]. First relativistic calculations of dimers Hg–Au and E112–Au indicate a lower, but still sizeable binding energy of the 112–Au dimer [24]. Therefore, current experiments focus on the property whether E112 also forms strong metal bonds with Au or whether E112 is so inert, that it behaves more like a heavy noble gas such as Rn.

Similar considerations apply to E114, which also has a higher ionization potential and no electron affinity, rendering it chemically less metallic and more inert compared to its lighter homolog Pb. Qualitatively these trends

were realized early on, already 1975 Pitzer published a short paper with the title "Are elements 112, 114, and 118 relatively inert gases?" [25]. Molecules of the type MX_4 (X = F, Cl) were calculated to be thermodynamically stable for M = Pb, whereas with M = E114 the +2 oxidation state will be favored [26].

Experimental Techniques

A chemistry experiment with a transactinide element can be divided in four basic steps: synthesis of the transactinide element; rapid transport of the synthesized nuclide to the chemical apparatus, fast chemical isolation of the desired nuclide and preparation of a sample suitable for nuclear spectroscopy, and, detection of the nuclide via its characteristic nuclear decay properties.

In order to gain access to the longer-lived isotopes of transactinide elements, exotic, highly radioactive target nuclides such as ^{244}Pu, ^{243}Am, ^{248}Cm, ^{249}Bk, ^{249}Cf, or ^{254}Es are bombarded with intense heavy ion beams such as ^{18}O, ^{22}Ne, ^{26}Mg, or ^{48}Ca. On the one hand as intense beams as possible are to be used; on the other hand the destruction of the very valuable and highly radioactive targets has to be avoided. A rotating ^{248}Cm target with a rotating vacuum window that can stand pressure differences of up to 1.5 atm has recently been used in heavy element chemistry experiments at the Gesellschaft für Schwerionenforschung (GSI). This rotating target carrying up to 6 mg of target material has allowed the use of high-intensity beams for heavy element chemistry experiments [9]. A picture of a rotating ^{248}Cm target after irradiation with up to 1 pμA of a ^{26}Mg beam (a factor of four larger than possible with a fixed target) is shown in Figure 3. The target wheel is synchronized with the time structure of the UNILAC in order to spread one beam pulse over the area of one target segment.

Figure 3. *The GSI rotating target wheel.*

Reaction products recoiling out of the target are stopped in a recoil chamber filled with helium gas. Non-volatile products are adsorbed on aerosol particles of about 100 nm diameter and transported through a capillary over relatively long distances to the chemistry apparatus. As aerosol materials potassium chloride (KCl) or carbon are often used. Aerosol particles of suitable size can be generated by sublimation of KCl that is heated in flowing He to about 640°C. Carbon aerosols are generated by spark discharge in flowing He. Unfortunately, high transportation yields cannot be reliably maintained over long time periods, also the yield is strongly dependent on the beam current and usually decreasing with increasing beam intensities. Sufficiently volatile reaction products such as Hg or E112 can be transported directly with the flowing gas. In experiments with Hs, recoiling atoms were converted *in-situ* with an admixture of O_2 gas to the volatile HsO_4.

Basically, four different approaches that involve the direct detection of the nuclear decay of the isolated nuclides have been successful in studying the chemical properties of transactinide elements. Two of the systems work in the liquid phase, whereas the other two are designed to investigate volatile transactinide compounds in the gas phase.

The predominant share of today's knowledge about the chemical behavior of Rf, Db, and Sg in aqueous solution was obtained with the **A**utomated **R**apid **C**hemistry **A**pparatus (ARCA). This micro-computer controlled set-up allows fast repetitive separations on miniaturized chromatography columns. Depending on the chemistry, the columns are filled with ion exchange resin or organic extractants on an inert support material. Often several thousand separations are performed. After chemical separation the fraction containing the transactinide element is evaporated and the sample placed in an α-/SF spectroscopy system. This last step, which was performed manually, has now also been automated in a set-up called AIDA developed in Japan. A schematic of this apparatus is shown in Figure 4.

A continuously operating liquid-liquid extraction system using miniaturized centrifuges and liquid scintillation flow through detection cells (SISAK) was recently successful to separate and identify 4-s ^{257}Rf [28]. The latest version of SISAK is very well adapted to study nuclides with half-lives as short as 1 s. In order to suppress the large background created by β-particles, a recoil chamber was coupled to the **B**erkeley **G**as-filled **S**eparator (BGS). Coupling a chemistry set-up with a recoil separator may open new frontiers in direct chemical reactions with a large variety of compounds, because one no-longer has to deal with the harsh ionizing

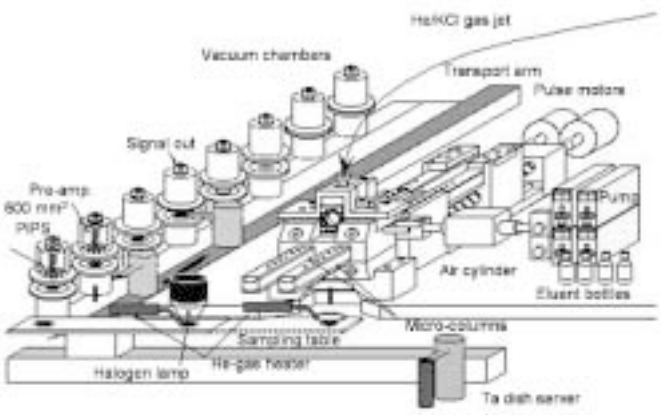

Figure 4. *Schematic of the **A**utomatic **I**on exchange separation apparatus coupled with the **D**etection System for **A**lpha Spectroscopy (AIDA) [27].*

conditions created by the passage of the primary beam. Furthermore, contaminants that cannot be effectively removed due to their chemical similarity to SHE, such as Po or Rn isotopes, are largely removed by the recoil separator.

In order to study elements beyond Sg, faster and much more efficient chemistry set-ups had to be used. Such systems are gas-phase chromatographic separations. Because transactinide nuclei are usually stopped in gas, a fast and efficient link to a gas chromatography system can be established; either by direct transport of volatile species or volatile compounds that were formed *in-situ* in the recoil chamber, or by a transport with aerosol particles. Despite the fact that the transition metals (groups 4 to 11) are very refractory, there exist few stable inorganic compounds that are appreciably volatile at experimentally manageable temperatures below 1100°C. These are the halides and oxyhalides of groups 4 to 7, the oxide hydroxides of groups 6, 7, and the oxides of group 8. Moreover, elements 112 to 118 are expected to be rather volatile in the elemental state and thus gas-phase separations will play a crucial role in investigating the chemical properties. Early on, gas-phase chemistry played an important role in the investigations of SHE. The technique was pioneered by Zvara and co-workers in Dubna to investigate Rf- and Db-halides that were formed *in-situ* behind the target and detected by latent fission tacks left in a thermochromatography column [9].

Later the **O**n-**L**ine **G**as-chemistry **A**pparatus (OLGA) was developed and successfully used to study halides and oxyhalides of elements Rf [9], Db [9], Sg [12], and also Bh [13]. A schematic of the OLGA set-up coupled to the **Ro**tating wheel **M**ultidetector **A**nalyzer (ROMA) is shown in Figure 5. Aerosols carrying reaction products form the target to the OLGA set-up are collected on a quartz wool plug inside the reaction oven kept at 1000°C. Reactive gases are introduced in order to form volatile compounds. The chromatographic separation takes place downstream in the adjoining isothermal section of the column. At isothermal temperatures ≥ 300°C most of the halides and oxyhalides of Rf, Db, Sg, and Bh are volatile and travel trough the column essentially without delay, whereas less volatile compounds are retained much longer and are removed by decay of the interfering nuclide. At the exit of the column the isolated molecules are attached to new aerosol particles and transported to a detection system. Thus, all investigated nuclides were unambiguously identified by registering α-particle decay chains.

The OLGA set-up was sensitive to cross sections of the order of 100 pb. In order to assess nuclides that are produced with few picobarn cross sections

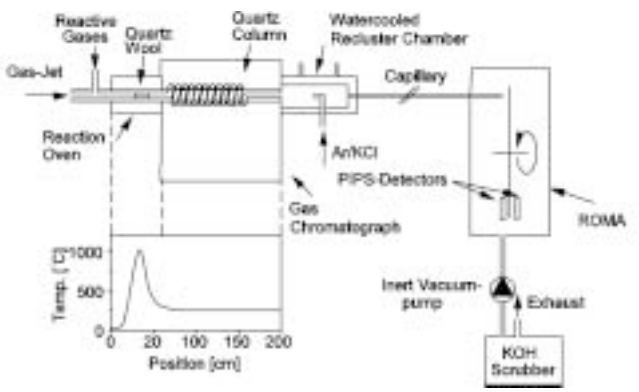

Figure 5. *Schematic of the OLGA set-up coupled to the ROMA detection system.*

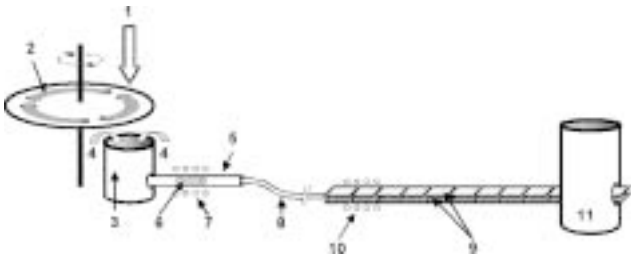

Figure 6. *The beam (1) passes through the rotating vacuum window and the target (2) assembly. Hs nuclei formed in fusion reactions recoil out of the target into a gas volume (3) and are flushed with a He/O_2 mixture (4) to a quartz column (5) containing a quartz wool plug (6) heated to 600°C by an oven (7). There, Hs is converted to HsO_4, which is volatile at room temperature and transported with the gas flow through a perfluoroalkoxy (PFA) capillary (8) to the **C**ryo **O**n-**L**ine **D**etector (COLD) registering the nuclear decay (α- and spontaneous fission) of the Hs nuclides. The array consisted of 36 detectors arranged in 12 pairs (9), each detector pair consisted of 3 PIN diode sandwiches. Always 3 individual PIN diodes (top and bottom) were electrically coupled. A thermostat (10) kept the entrance of the array at 20°C; the exit was cooled to 170°C by means of liquid nitrogen (11). Depending on the volatility of HsO_4, the molecules adsorbed at a characteristic temperature. Figure from Ref. [14].*

the overall efficiency had to be improved by at least one order of magnitude. This was accomplished by introducing the *in-situ* formation of volatile compounds and their condensation and detection in a thermochromatography detector, as in the early experiments by Zvara. Instead of an isothermal temperature profile as in OLGA, a negative longitudinal temperature gradient is established along the column. Thus, compounds are deposited in the chromatography column according to their volatility, forming distinct deposition peaks. If the column consists of silicon detectors then the nuclear decay of the separated nuclide can be registered. The detector number indicates the temperature at which the volatile compound was deposited. Thus, every detected nuclide reveals also chemical information. A schematic of the **I**n-situ **V**olatilization and **O**n-line detection apparatus (IVO) [29] is shown in Figure 6. The IVO set-up was successfully used to study the chemical properties of HsO_4 [14]. The overall efficiency (including detection of a complete 3 member α-particle decay chain) is of the order of 30–50%.

Similar set-ups were used in first attempts to chemically identify E112. If E112 is chemically similar to Hg it should adsorb on Au or Pd surfaces. In test experiments short-lived Hg isotopes could be isolated in the elemental form from other reaction products and transported in He quantitatively through a 30 m long Teflon™ capillary at room temperature. Adsorption of Hg nuclides on silicon detectors, proved experimentally not feasible, because Hg was adsorbed on quartz surfaces only at temperatures of –150°C and below. However, Hg adsorbed quantitatively on Au, Pt, and Pd surfaces at room temperature. As little as 1 cm^2 of Au or Pd surface was sufficient to adsorb Hg atoms nearly quantitatively from a stream of 1 l/min He [16]. Therefore, detector chambers containing a pair of Au- or Pd-coated PIPS detectors were constructed. Eight detector chambers (6 Au and 2 Pd) were connected in series by Teflon™ tubing. The detector chambers were positioned inside an assembly of 84 ^{3}He-filled neutron detectors (in a polyethylen moderator) in order to simultaneously detect neutrons accompanying spontaneous fission events (see Figure 7) [16,17]. In the latest experiment aiming at measuring the volatility of E112, one row of the silicon detectors of the COLD detector was removed and replaced by a Au surface. A negative temperature gradient was established reaching from room temperature down to –187°C [18].

Recent Results on the Chemistry of Hassium

In the course of an experiment to produce the nuclides ^{269,270}Hs in the reaction ^{248}Cm(^{26}Mg, 4n) and ^{248}Cm(^{26}Mg, 5n) conducted in May of 2001 at the GSI, valid data was collected during 64.2 h [8,14]. During this time $1.0 \cdot 10^{18}$ ^{26}Mg beam particles passed through the ^{248}Cm target. The IVO set-up was used to synthesize volatile HsO_4, which were adsorbed in the COLD detector. Only α-lines originating from ^{211}At, ^{219,220}Rn and their decay products were identified. Whereas ^{211}At and its decay daughter ^{211}Po were deposited mainly in the first two detectors, ^{219,220}Rn, and their decay products accumulated in the last three detectors, where the temperature was sufficiently low to partly adsorb Rn. During the experiment, seven correlated decay chains were detected (see Figure 8). All decay chains were

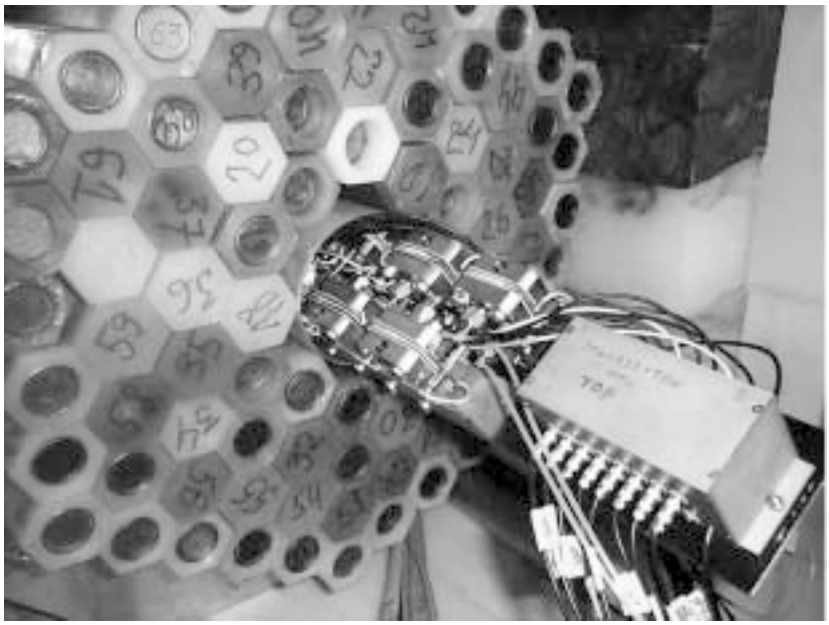

Figure 7. *Detector arrangement for the detection of ^{283}112 consisting of pairs of Au- and Pd-coated PIPS detectors inside an assembly of 84 ^{3}He-filled neutron detectors [16].*

observed in detectors 2 through 4 and were assigned to the decay of either ^{269}Hs or the yet unknown ^{270}Hs. The characteristics of the three decay chains agreed very well with the decay properties of ^{269}Hs and its daughter nuclides observed in two decay chains of ^{277}112 [5]. The unusual α-decay energy of 8.52 MeV, which fits well into the systematic of ground-state α-decay energies, as well as a rather large spontaneous fission branch could be confirmed for the nuclide ^{261}Rf. The previously well-established decay properties of ^{261}Rf ($T_{1/2}$ = 78 s, E_α = 8.28 MeV, SF < 10%) must therefore be assigned to a long-lived isomeric state. Two additional decay chains were tentatively attributed to the decay of ^{270}Hs. The last two decay chains were incomplete and a definite assignment to ^{269}Hs or ^{270}Hs could not be made. No additional three-member decay chains with a total length of ≤ 300 s were registered in detectors 2 to 10. The background count-rate of α-particles with energies between 8.0 and 9.5 MeV was about 0.6 h^{-1} per detector, leading to very low probabilities of $\leq 7 \times 10^{-5}$ and $\leq 2 \times 10^{-3}$ for any of the first five chains and any of the last two chains, respectively, being of random origin. In addition, four fission fragments with energies > 50 MeV that were not correlated with a preceding α-particle were registered in detectors 2 through 4. Assuming an overall efficiency of ≈ 40%, a production cross section of 4 pb for α-decaying ^{270}Hs and of 6 pb for α-decaying ^{269}Hs was calculated at a beam energy of 143.7-146.8 MeV (with an estimated uncertainty accuracy of a factor of ≈ 3).

The longitudinal distribution of the 7 decay chains originating from Hs is depicted in Figure 9. The maximum of the Hs distribution was found at a temperature of 44 ± 6°C. The distribution of $^{172}OsO_4$ ($T_{1/2}$ = 19.2 s) measured before and after the experiment showed a maximum in detector 6 at a deposition temperature of 82 ± 7°C. The higher deposition temperature of about 40°C and the thus about 7 kJ/mol higher adsorption enthalpy seems to indicate a slightly lower volatility of HsO_4 compared to its lighter homolog OsO_4. This experimental result was somewhat unexpected because according to both, classical extrapolations and relativistic molecular calculations, HsO_4 was predicted to be about as volatile as OsO_4. Nevertheless, the high volatility of the Hs oxide species clearly suggests that it is HsO_4 because, by analogy with the known properties of the Os oxides, all other Hs oxides are expected to be much less volatile and unable to reach the detector system. The observed formation of a volatile Hs oxide (very likely HsO_4) provides strong experimental evidence that Hs behaves chemically as an ordinary member of group 8 of the Periodic Table.

Recent Results on the Chemistry of E112

A first attempt to chemically identify one of the long-lived isotopes of element 112, namely ^{283}112 (SF, $T_{1/2}$ ≈ 3 m) [30], in the elemental state was made by Yakushev et al. [16] using the ^{48}Ca+ ^{238}U production reaction. It should be noted that in very recent experiments at the Dubna gas-filled separator, this long-lived SF activity could no longer be identified. Instead ^{283}112 decayed by α-particle emission (E_α = 9.54 MeV, $T_{1/2}$ ≈ 6 s) to short-lived ^{279}110 (SF, $T_{1/2}$ ≈ 0.3 s) [15].

In an experiment conducted in January 2000 a total beam dose of $6.85 \cdot 10^{17}$ ^{48}Ca ions was accumulated. The chemical yield for the simultaneously produced ^{185}Hg ($T_{1/2}$ = 49 s) was 80%. If element 112 behaved

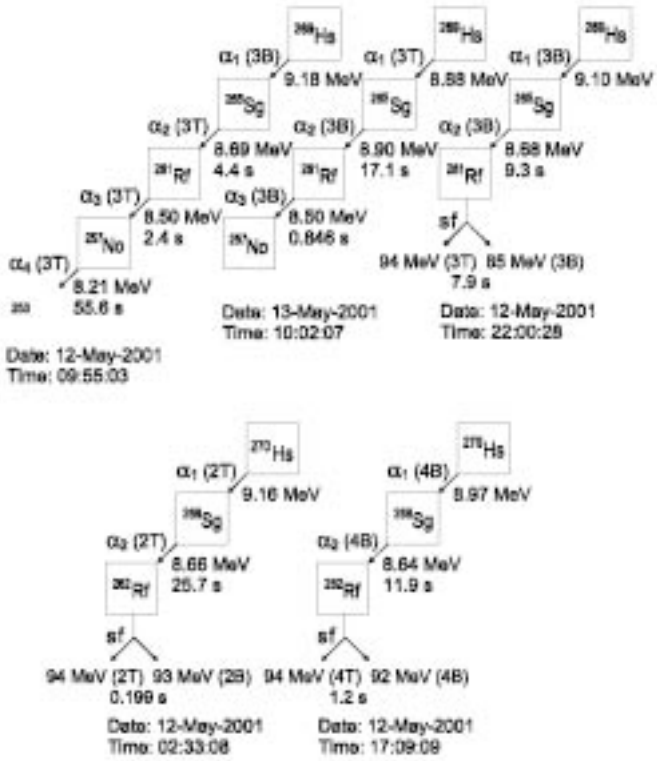

Figure 8. *Observed decay chains attributed to the decay of ^{269}Hs and ^{270}Hs produced in the reaction ^{26}Mg + ^{248}Cm [8].*

chemically like Hg and all efficiencies measured for Hg were also valid for element 112, detection of 2–4 SF events could be expected assuming the cross-section value for the production of ^{283}112 measured in [16]. However, no SF events were observed. Therefore, no unambiguous answer as to the chemical and physical properties of element 112 was obtained.

In a next experiment, the question whether element 112 remained in the gas phase and passed over the Au surfaces was addressed [17]. Therefore, a special ionization chamber to measure SF fragments of nuclei remaining in the gas was added at the exit of the Au coated PIPS detector array. A total beam dose of $2.8 \cdot 10^{18}$ ^{48}Ca ions was accumulated. Again no SF events were registered on the Au and Pd coated PIPS detectors, confirming the result of the first experiment. However, 8 SF events accompanied by neutrons were registered in the ionization chamber, whereas only one background count was expected. Therefore, the majority of the SF events were attributed to the decay of a nuclide of element 112, since there are no other known volatile nuclides decaying by SF. From these experiments it appears that the interaction of element 112 with an Au or Pd surface is much weaker than for Hg. In the light of the latest results from Dubna the question arises whether the observed SF events could be attributed to the decay of ^{279}Ds, the daughter of 6 s ^{283}112. Calculations of the transport time of a volatile nuclide from the target to the ionization chamber show that indeed this scenario cannot be excluded with certainty, but the experiment was designed to be most sensitive for a 3 min nuclide.

Obviously, in a next step, the adsorption temperature of element 112 on Au surfaces has to be measured experimentally. This was done with a modified version of the cryo thermochromatography detector in an experiment conducted recently at the GSI [18]. A 1.5 mg/cm^2 thick ^{238}U target was bombarded with $2.8 \cdot 10^{18}$ ^{48}Ca particles. A total of 11 events with energies > 40 MeV were registered with an estimated background of about 3 events. Seven events were registered at the cold end of the detector where also Rn was deposited. However, none of these events was correlated with a preceding α-particle. Therefore, the detected events cannot yet be conclusively attributed to the decay of E112 or its daughter.

Summary and Outlook

The spectacular results obtained at Flerov Laboratory in Dubna using ^{48}Ca ion beams and actinide targets to synthesize isotopes of elements 112, 114, 115, and 116 [31] give chemists the historic opportunity to experimentally investigate the chemistry of even the heaviest known elements. Especially because some of the nuclides and their decay products seem to have half-lives of the order of seconds to even hours. In the last couple years, chemists have made a quantum leap and are now working with nuclides that can be produced with picobarn (10^{-36} cm^2) cross sections only, as demonstrated by the first chemical investigations of hassium. There are indications that the chemical investigation of E112 and also E114 seem to reveal strong relativistic effects that significantly alter the chemical behavior of these elements

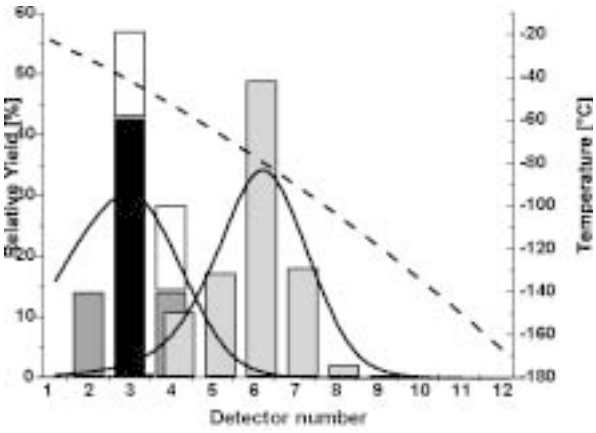

Figure 9. *Relative yields of HsO_4 and OsO_4 for each of the 12 detector pairs. Measured values are represented by bars: $^{269}HsO_4$: black; $^{270}HsO_4$: dark grey; $^{269\ or\ 270}HsO_4$: white; $^{172}OsO_4$: light grey. The dashed line indicates the temperature profile (right-hand scale). The maxima of the deposition distributions were evaluated as –44 ± 6°C for HsO_4 and –82 ± 7°C for OsO_4. Solid lines represent results of a Monte Carlo simulation of the adsorption process.*

compared to their lighter homologs. The unambiguous identification of the separated nuclides by measuring their decay properties yields additional valuable information about the nuclear structure of SHE. In order to reduce interferences from the plasma created by the beam and from undesired by-products of the nuclear reaction, chemists are investigating possibilities to couple their equipment with recoil separators. First experiments with the recoil transfer chamber coupled to the BGS were very successful. At the GSI components of the dismantled HECK separator [32] are being used to set up a dedicated separator that suits the needs of chemistry.

Due to the decreasing production cross sections, chemists also have to rely on future accelerators that will deliver even higher beam intensities. A substantial amount of beam time is required for each heavy element experiment. Target designs that allow the irradiation of exotic radioactive materials with highest possible beam intensities must be developed. Intense, neutron-rich radioactive heavy ion beams will be the only way to approach the predicted $N = 184$ neutron shell and produce long-lived SHE. Prospects to experimentally study the chemical properties of all currently known elements in the Periodic Table, even though only single atoms can be produced, are fascinating and challenge our creativity.

References

1. G. T. Seaborg, W. D. Loveland, The elements Beyond Uranium, John Wiley & Sons, Inc., New York (1990).
2. Z. Patyk et al., *Nucl. Phys.* A502 (1989) 591c.
3. Yu. A. Lazarev et al., *Phys. Rev. Lett.* 73 (1994) 624.
4. P. A. Wilk et al., *Phys. Rev. Lett.* 85 (2000) 2697.
5. S. Hofmann et al., *Eur. Phys. J.* A14 (2002) 147.
6. A. Türler et al., *Phys. Rev.* C57 (1998) 1648.
7. A. Türler et al., *Eur. Phys. J.* A15 (2002) 271.
8. A. Türler et al., *Eur. Phys. J.* A17 (2003) 505.
9. M. Schädel, Ed., The Chemistry of Superheavy Elements, Kluwer Academic Publisher, Dordrecht (2003).
10. H. Haba et al., *J. Am. Chem. Soc.* 126 (2004) 5219.
11. J. V. Kratz, *Pure Appl. Chem.* 75 (2003) 103.
12. M. Schädel et al., *Nature* 388 (1997) 55.
13. R. Eichler et al., *Nature* 407 (2000) 63.
14. Ch. E. Düllmann et al., *Nature* 418 (2002) 859.
15. Yu. Ts. Oganessian et al., *Phys. Rev.* C69 (2004) 054607.
16. A.B. Yakushev et al., *Radiochim. Acta* 89 (2001) 743.
17. A.B. Yakushev et al., *Radiochim. Acta* 91 (2003) 433.
18. H.W. Gäggeler et al., *Nucl. Phys.* A734 (2004) 208.
19. P. Pyykkö, J. Desclaux, *Acc. Chem. Res.* 12 (1979) 276.
20. V. G. Pershina, *Chem. Rev.* 96 (1996) 1977.
21. P. Schwerdtfeger, M. Seth, Encyclopedia of Computational Chemistry, Vol. 4 (Eds. P. von Ragué Schleyer et al.) John Wiley & Sons, Inc., New York (1998) pp. 2480–2499.
22. V. Pershina et al., *J. Chem. Phys.* 115 (2001) 792.
23. E. Eliav et al., *Phys. Rev. Lett.* 73 (1994) 3203.
24. V. Pershina et al., *Chem. Phys. Lett.* 365 (2002) 176.
25. K. S. Pitzer, *J. Chem. Phys.* 63 (1975) 1032.
26. M. Seth et al., *Angew. Chem. Int. Ed.* 37 (1998) 2493.
27. Y. Nagame, private communication.
28. J. P. Omtvedt et al., *J. Nucl. Radiochem. Sci.* 3 (2002) 121.
29. Ch. E. Düllmann et al., *Nucl. Instr. Meth.* A479 (2002) 631.
30. Yu. Ts. Oganessian et al., *Nature* 400 (1999) 242.
31. Yu. Ts. Oganessian, contribution to the TAN´03 Conference, Napa 17–20 November 2003.
32. V. Ninov et al., *Nucl. Instr. Meth.* A357 (1995) 486.

Developments in Spectroscopic Studies of Deformed Superheavy Nuclei

P. A. Butler
PH-ISOLDE, CERN, CH - 1211 Geneva 23, Switzerland [1]

M. Leino
Department of Physics, University of Jyväskylä, 40014 Jyväskylä, Finland

Introduction

The search for new elements and the study of their structure and decay properties has been in the forefront of nuclear physics for decades, especially since detailed theoretical predictions of the existence of superheavy elements (SHE) appeared in the mid 1960s. The heaviest elements offer a unique possibility to study the effective nuclear interaction because of the delicate interplay of attractive nuclear and disruptive Coulomb forces. Nuclides with proton number higher than 104 (rutherfordium, Rf) or so survive against fission only because of quantum effects that build up a fission barrier. The understanding of the structure of SHE is essential for the development of mean field theories that are used to predict nuclear properties far from stability. Forty years ago the first attempts to predict nuclear shell structure beyond ^{208}Pb were made using macroscopic-microscopic models. The Nilsson model and later refinements using more realistic charge and mass distributions predict that there will be significant shell corrections giving rise to enhanced stability to an "island" of near-spherical nuclei with Z~114 and N~184. This has remained the only prediction for magic numbers in this mass region until the recent application of self-consistent microscopic theories to SHE. The self-consistent theories have consistently predicted different positions [1–3] for the shell closures: Skyrme-Hartree-Fock parameterisations give Z~126, N = 184 whereas relativistic mean fields give Z~120, N~172. These differences arise primarily because of the close level spacing for quantum systems containing a large number of nucleons so that changes in the mean field description give a significant reordering of states having different quantum numbers. This is illustrated in Figure 1, which shows that the shell correction energy for SHE is quite diffuse with proton and neutron number, as compared with the behavior at smaller magic numbers. The authors of the self-consistent theories have also found deficiencies in the treatment of surface properties in macroscopic-microscopic models, whereas differences between relativistic and non-relativistic models can be ascribed to differing spin-orbit potentials.

Since the early 1980s cold fusion evaporation reactions have been used to produce SHE, using targets in the immediate vicinity of ^{208}Pb [4]. The correlation method using long alpha decay chains provided not only certain identification of the products but also some structure information, limited by the very small statistics. In this way, elements 107–112 were synthesized at GSI, Darmstadt. The first four of these have been named, with the most recent assignment (darmstadtium) given to element 110 in December 2003. IUPAC has also given permission to name element 111, with 112 waiting for confirmation as the data are still judged to be inconclusive by IUPAC.

The reduction in cross section of (HI, 1n) reactions leading to progressively heavier elements is quite regular. Extrapolation to elements heavier than 112–113 suggests production rates that would require very long irradiations using presently available techniques. Somewhat surprisingly, returning to the use of actinide targets and warm or hot fusion reactions seems to have given a new boost to new element synthesis. During the last few years, experiments performed in Dubna have provided evidence for the production of elements 112–118 using this method. The drawback is that the decay chains end up in fission in an unknown region on the chart of nuclei, making it impossible to firmly identify the synthesized nuclides and thus making it difficult to draw conclusions concerning the nuclear structure of these nuclei.

[1]Permanent address: Oliver Lodge Laboratory, University of Liverpool, Liverpool L69 7ZE, UK.

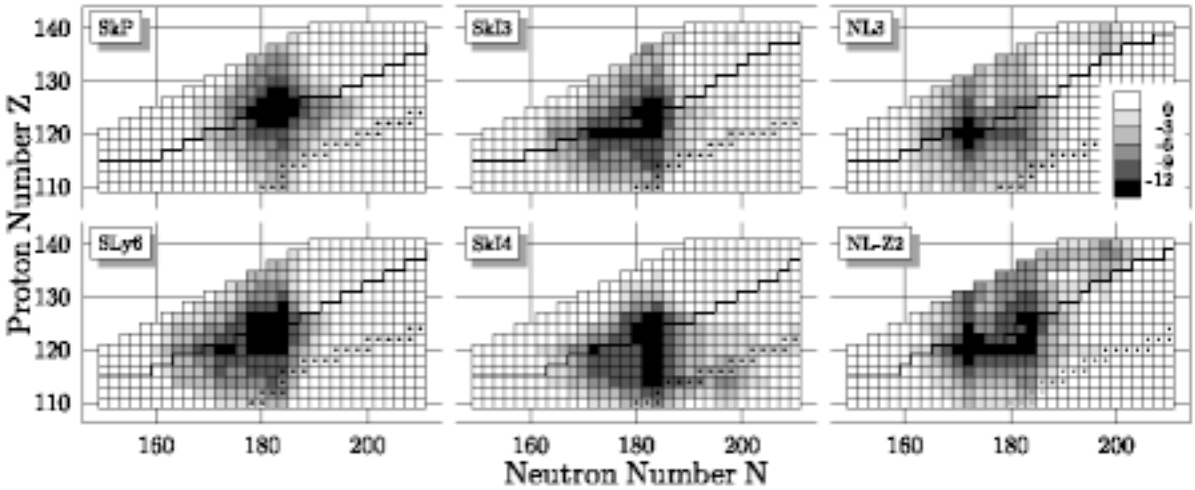

Figure 1. *Total shell correction (in MeV) calculated for spherical even-even nuclei around the expected island of stability around Z = 120 and N = 180. Taken from Ref. [3].*

The experiments described so far aim to measure the structure of SHE by direct measurement of the ground state properties of nuclei. Equally important information can come from the study of mid-shell deformed nuclei, because selected single particle orbitals that lie close to the spherical shell gap in SHE are close to the Fermi level in nuclei having large quadrupole deformation. In such nuclei, having Z~100, the microscopic contribution to the total nuclear energy, now coming from the lowering of single particle states in a deformed quantum system, still provides the essential stabilization against fission. The cross-section for the population of these nuclei is, however, many orders of magnitude higher than for Z > 112, so that detailed radioactive decay spectroscopy or in-beam spectroscopy becomes possible.

A very important step forward in structure studies was taken only a few years ago when the focal plane alpha detector setups of fast recoil separators were complemented with conversion electron and X-ray and gamma-ray spectrometers, allowing the extraction of much more information on spins and parities of nuclear states. Another leap was taken in 1998 when the first in-beam gamma-spectroscopy studies were performed on ^{254}No in Argonne and Jyväskylä.

Developments in Heavy Ion Spectroscopy

Most of present-day synthesis experiments and nuclear structure studies in the SHE region make use of fast and efficient online recoil separators to detect the products of complete fusion reactions using heavy ion beams and various stable or radioactive targets. The task of the recoil separator is to filter away the primary accelerator beam and the majority of unwanted reaction products (mostly fission for A > 180 nuclei). Their operation is based on the fact that fusion evaporation products recoil at close to zero degrees relative to the beam with nearly the full momentum of the heavy ion but with magnetic or electric rigidity that differs from that of the beam and the background particles. Because of the small production rates of the heaviest nuclei, high transmission through the separator is of primary importance so mass resolution has been sacrificed in their design in favor of efficiency. Identification of the products is usually based on the characteristics of their radioactive decay (usually α-decay) observed in the detector set-up surrounding the focal plane of the separator (Recoil Decay Tagging or RDT).

The focal plane detector system is invariably based on a position sensitive Si detector for the observation of the arrival and decay of the fusion evaporation products. The size of the detector is typically on the order of a few square cm. Upstream from this detector is usually a tunnel-like arrangement of additional Si detectors for observing α-particles and conversion electrons escaping backwards from the recoil implantation detector. This arrangement increases the efficiency for observing the full energy of α-particles to typically 80%.

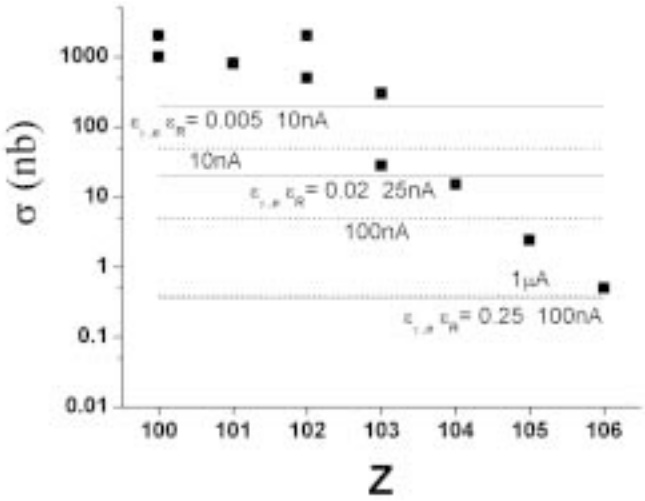

Figure 2. *Sensitivity of in-beam and decay spectroscopy experiments. Black squares are experimental cross sections for nuclei of interest. The solid line shows the limit of cross-section that can be studied in-beam; the dashed line the limit of cross-section of daughter nucleus populated by α-decay that can be studied. The three values of $\varepsilon_R \cdot \varepsilon_{\gamma,e}$ for in-beam measurements (0.005, 0.02, 0.25) correspond to JUROSPHERE/RITU or Gammasphere/FMA, JUROGAM/RITU, and in the future, AGATA/RITU, respectively.*

For in-beam experiments, two separators and associated detector systems have been used. The FMA at Argonne National Laboratory has been used in conjunction with the very efficient Gammasphere germanium detector system. The FMA has sufficient mass resolution to uniquely determine the mass number of fusion evaporation products in the heavy element region with high efficiency, typically of the order of 5–15%. The efficiency of Gammasphere at 1.3 MeV is approximately 10%. The BGO shields of Gammasphere provide the additional possibility of calorimetric measurements that have allowed the collection of groundbreaking information on the spin-entry distribution in the region close to ^{254}No.

The gas-filled RITU separator at JYFL, Jyväskylä, has an even higher transmission, typically 25–40%, due to its charge and velocity focusing characteristics. It has been operated in conjunction with various germanium detector arrays ranging in efficiency from 0.7% upward. The presently operating JUROGAM array, which consists of 43 Eurogam Phase 1 detectors, has a total efficiency of 4.5% at 1.3 MeV. The unique feature at JYFL is the possibility of for the first time recording conversion electrons in-beam using the RDT method. This has been made possible by joint Liverpool–Jyväskylä efforts in developing the SACRED electron spectrometer [5,6]. SACRED has an efficiency of approximately 10% for energies below 300 keV. The segmentation of the 28 mm diameter Si detector makes it possible to record electron-electron coincidences.

Recently, a new detector system called GREAT [7] was installed at the RITU focal plane. This versatile system allows, in addition to the observation of the arrival and the decay chain of the fusion product, the detection of escape α-particles, conversion electrons, β-decays, as well as X-rays and γ-rays using a segmented planar Ge detector and a large Ge clover detector. To facilitate readout of asynchronous data from the target-area and the focal plane detectors a new triggerless data acquisition system called TDR (Total Data Readout) was also developed [8].

The philosophy of spectroscopic measurements has been either to measure decay properties of nuclei in the focal plane, in which case the sensitivity of measurement is determined by the primary beam current, or to measure in-beam properties directly, in which case the sensitivity is determined by the product of the recoil separator efficiency (ε_R), the γ- or electron array efficiency ($\varepsilon_{\gamma,e}$) and the beam current. This is illustrated in Figure 2, which shows how nuclei of increasing Z can be studied by in-beam or decay spectroscopy.

Status of Current Research

A breakthrough for SHE studies using tagging techniques came from its application [9,10] to the reaction ^{208}Pb(^{48}Ca,2n)^{254}No, which has a cross-section of 2 μb. The experimental observation of the ground-state rotational band up to spin 18 was a significant find in that it confirmed the deformed nature of the mid-shell nucleus ^{254}No and demonstrated that the deformed shell stabilization against fission persists to high spin. Since then, experiments have been carried out to measure the rotational properties of the even-even nuclei ^{252,254}No and ^{250}Fm [11]. These nuclei have similar values of quadrupole deformation, β~0.28, and for ^{252}No a gradual upbend of the

dynamic moment of inertia is observed as compared to its isotonic and isotopic neighbors. Research efforts have also been directed to odd-mass systems that can reveal single particle properties near the Fermi surface. A severe experimental handicap in these studies arises from the internal conversion of the M1 transitions depopulating the strongly coupled rotational bands built on single particle states. In some cases that have been studied, such as ^{253}No and ^{255}Lr, the gamma-ray intensities are too weak to allow the extraction of quantitative information. Gamma-ray measurements of odd mass nuclei now focus on specific cases such as ^{251}Md for which either the M1 branching is weak (cancellation of single particle and rotational g-factors) or the signature partners of the rotational band are decoupled (K = 1/2 ground state).

Another promising approach is to study bands built on multi-quasiparticle states in these heavy nuclei. A recent study [12] of prompt conversion electrons emitted by excited ^{254}No nuclei has revealed that a large fraction (40%) of the decays proceed through high-K bands that probably terminate in isomeric states. The high electron multiplicity of these decay paths give rise to a quasi-continuous background. This background dominates the observed electron spectrum as can be seen in Figure 3. Evidence for the presence of a long-lived isomer in ^{254}No has been presented thirty years ago and efforts are underway to quantify the character (excitation energy, spin, parity) of low-lying isomers in this mass region.

Spectroscopic information can also be obtained by measuring the decay properties of excited states populated by radioactive decay of the parent nucleus. If the parent is sufficiently long-lived it can be chemically separated and several collective bands in ^{256}Fm, fed by the decay of a 7$^-$ isomer, have been classified. This isomer is populated by the beta-decay of its parent ^{256}Es. For shorter-lived parent nuclei, electromagnetic in-flight separation is necessary. Although the cross-section for the population of the parent is smaller by one or two orders of magnitude than that of the daughter nucleus being investigated, there are two compensating factors: the measurements are made in the low background environment of the recoil separator and higher beam currents can be employed if direct radiation from the target is not detected. Recent experiments [11] using GREAT (RITU) and similar instrumentation in the focal plane of SHIP have observed the lowest three members of the rotational band in ^{249}Fm populated following the alpha decay of ^{253}No.

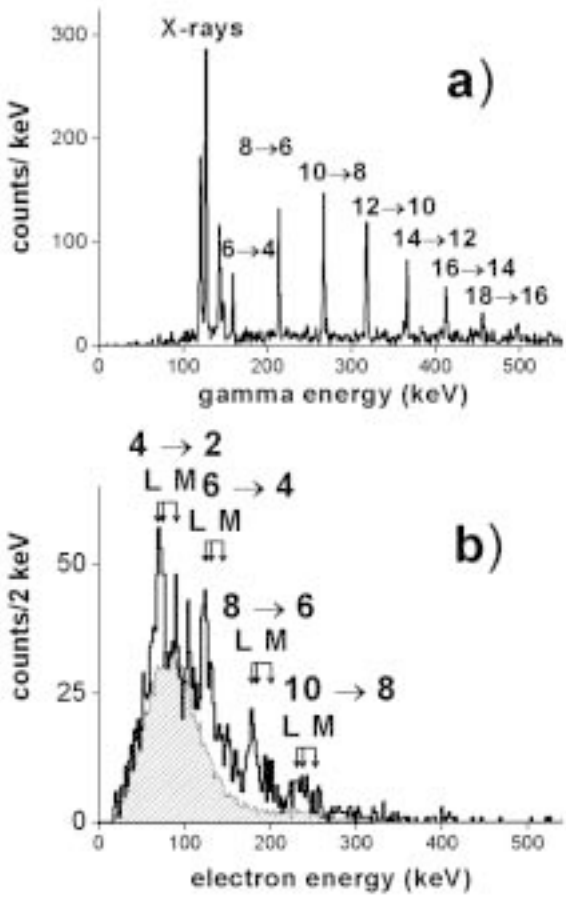

Figure 3. *Comparison of in-beam (a) γ-ray spectrum (courtesy of S. Eeckhardt) and (b) conversion electron spectrum following the reaction ^{208}Pb(^{48}Ca, 2n)^{254}No. In the latter the shaded region is a simulation assuming that the nucleus decays by many M1 paths built on high-K states [12].*

Perspectives

The sensitivity of current state-of-

the-art in-beam gamma-ray spectrometers such as JUROGAM and decay spectrometers such as GREAT, used in conjunction with recoil separators such as RITU, is such that in-beam or decay spectroscopy is possible for Z = 104 (Rf), populated directly with cross-sections of order 10 nb, or by α-decay with $\sigma \sim 500$ pb. In-beam studies of odd-mass nuclei and K-isomer bands in even-even nuclei await the construction of hybrid electron–gamma spectrometers for which the absolute efficiency for either radiation is 10% or better. The range of accessible nuclei can be extended by the use of radioactive targets, although the recoil efficiency for the asymmetric reactions will be smaller than for the cold fusion reactions employed at present. The use of radioactive beams will also extend the range of nuclei that can be studied, and sufficient beam intensities of neutron-rich projectiles that neighbor ^{48}Ca such as ^{43}Ar and ^{46}K will be available from third generation radioactive beam facilities such as EURISOL and RIA.

References

1. S. Cwiok et al., *Nucl. Phys.* A611, (1996) 211.
2. A. T. Kruppa et al., *Phys. Rev.* C61, (2000) 034313.
3. M. Bender et al., *Phys. Lett.* B515 (2001) 42.
4. P. Armbruster, *Annu. Rev. Nucl. Part. Sci.* 50 (2000) 411.
5. P. A. Butler et al., *Nucl. Instr. Meth.* A381, (1996) 433.
6. H. Kankaanpää et al., *Nucl. Instr. Meth.* A, A534, (2004) 503.
7. R. D. Page et al., *Nucl. Instr. Meth.* B204 (2003) 634.
8. I. Lazarus et al., *IEEE Trans. Nucl. Sci.* 48 (2001) 567.
9. P. Reiter et al., *Phys. Rev. Lett.* 82, (1999) 509.
10. M. Leino et al., *Eur. Phys.* J. A6, (1999) 63.
11. R.-D. Herzberg, *J. Phys. G: Nucl. Part Phys.* 30, (2004) R123.
12. P.A. Butler et al., *Phys. Rev. Lett.* 89, (2002) 202501.

P. A. Butler
PH-ISOLDE, CERN, CH-1211 Geneva 23, Switzerland

M. Leino
Department of Physics, University of Jyväskylä, Finland

Application of Low Energy Spin Polarized Radioactive Ion Beams in Condensed Matter Research

Introduction

The new ISAC facility at TRIUMF (Canada), produces some of the world's most intense radioactive ion beams (RIBs). Although the primary scientific motivation for these facilities lies in nuclear physics and nuclear astrophysics, RIBs also have applications in condensed matter (CM). Many pioneering CM experiments have already been performed at the ISOLDE facility (CERN). Continuing on this path at ISAC we have recently polarized a beam of $^{8}Li^{+}$ to be used as a magnetic probe of ultra-thin films and interfaces. We report here on progress in developing this new application of low energy RIBs, which is based on the technique of β-detected nuclear magnetic resonance (β-NMR).

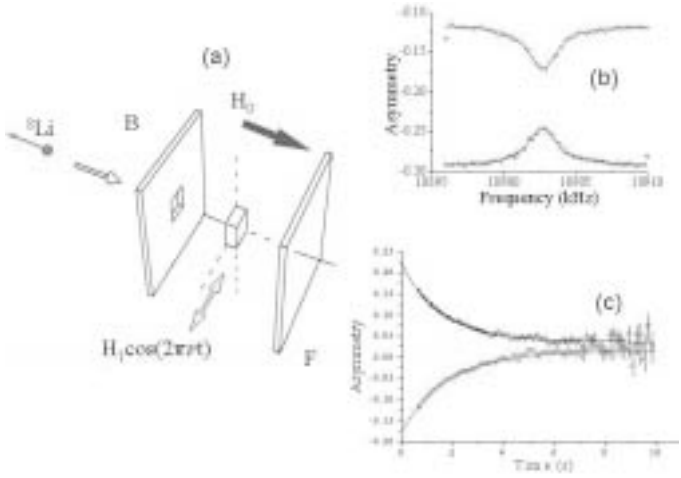

Figure 1. *(a) A schematic of a* β*-NMR experiment. The initial polarization can either be perpendicular to the beam direction or parallel as shown here. Plastic scintillation detectors (F and B) are used to monitor the* ?*- decay asymmetry as a function either of (b) RF frequency with a continuous beam or (c) time with a pulsed beam. The two different curves in (b) and (c) correspond to two different beam helicities.*

Conventional NMR is a powerful technique for probing the local electric/magnetic properties of materials [1] However, NMR typically requires a large number (10^{18}) of nuclear spins to generate a signal. Consequently it is most widely used in studies of bulk materials. A much greater sensitivity can be obtained with β-NMR where the signal is detected through the β-decay of a polarized radioactive nucleus. For example, in the case of ^{8}Li, which has a mean lifetime of 1.2 s, an energetic electron is emitted preferentially in the direction opposite to the nuclear polarization. Such β-decay anisotropy was first used to demonstrate parity violation in weak interactions in 1957 [2]. Since then β-NMR has been used extensively to measure nuclear moments of unstable isotopes. In condensed matter β-NMR allows one to simulate the behavior of stable isotopes with unprecedented sensitivity [4,5] For example, in semiconductors a radioactive nucleus is ideally suited to characterizing the behavior of an isolated impurity where conventional NMR lacks the required sensitivity [6]. Intense low energy beams of highly polarized ions, now available at ISAC, present new opportunities in condensed matter research. In particular, because only about 10^{7} spins are needed to generate a β-NMR signal, the method is well suited for studies of nano-structures and ultra-thin films where there are few host nuclear spins. Furthermore, with the unique polarized ion beam now at ISAC, it is possible to vary the mean depth of implantation on a lengthscale of nanometers. The scientific applications are similar to what is now possible with low energy muon beams [8]. However, the positive muon and a radioactive nucleus are very different probes and thus provide complementary information [9]. In addition RIBs from an ISOL target are naturally created at low energy and can be orders of magnitude more intense than a low energy muon beam.

β-NMR has close similarities to both muon spin rotation and conventional NMR. The two basic observables are the spin precession frequency and spin relaxation rate, both of which are used to monitor the local electronic/magnetic environment. A schematic of a typical β-NMR setup is shown in Figure 1a. Similar to muon

spin rotation, the experiment is carried out by implanting spin polarized particles (ions) into the sample. A static external magnetic field (H_0) is applied along the initial spin polarization direction $\hat{z}$ while an oscillating transverse magnetic field ($H_1 \cos 2\pi\nu t$) is stepped through a range of frequencies around the Larmor frequency of the nucleus ($\nu_L = \gamma B$), where B is the local magnetic field at the nuclear site and γ is the gyromagnetic ratio. The time averaged nuclear polarization P_z, is directly proportional to the β-decay asymmetry:

$$AP_z(\nu) = \frac{F(\nu) - B(\nu)}{F(\nu) + B(\nu)} \quad (1)$$

where $F(\nu)$ and $B(\nu)$ are the number of counts in the F and B detectors at frequency ν (corrected for the slightly different efficiencies of the detectors). The proportionality constant $A \approx 0.15$ depends on the beam polarization, β-decay characteristics, and various instrumental parameters. The resonances are detected by measuring the β-decay asymmetry as a function of ν. A decrease in P_z occurs when ν is matched to the nuclear spin splitting subject to the usual magnetic dipole selection rule $\Delta m = \pm 1$ (see Figure 1b). The position of the β-NMR resonance is a precise measure of the local magnetic field at the site of the nucleus which depends on the local electronic structure and static spin susceptibility of those electrons. Alternatively one can measure the $1/T_1$ nuclear spin relaxation rate by implanting a short beam pulse and measuring the time evolution of the polarization (see Figure 1c). The spin relaxation rate is sensitive to the electron spin dynamics. Of course in general the presence of the impurity will alter the local electronic structure. However, studies with muons have shown that the temperature dependence and magnetic field dependence of the frequency shifts and spin relaxation rates are often the same as those detected using the host nuclear spins.

Recently we have also performed the first zero field β-NQR (Nuclear Quadrupole Resonance) experiment, which is done in the absence of a static magnetic field (H_0=0). It is well known that if a nucleus with an electric quadrupole moment, such as ^{8}Li , rests in a crystalline site with non-cubic symmetry, there will be a quadrupolar splitting of the nuclear spin levels even in zero external magnetic field. One can induce transitions between these levels with the oscillating magnetic field (H_1), and thereby alter the nuclear spin population. The ability to perform magnetic resonance in zero applied field has important applications for studies on exotic magnetism and superconductivity. It is also remarkable that the ^{8}L? NQR resonances are narrow (few kHz) and easily observed at acoustic frequencies. Recall that in conventional NQR the signal to noise ratio degrades rapidly with decreasing frequency, and has a practical lower limit of a few MHz.

The β-NMR and β-NQR results from ISAC demonstrate that a low energy polarized beam of ^{8}L? can be used as a sensitive probe of the magnetic properties of thin films and interfaces where it is very difficult to obtain equivalent information with conventional NMR. Although the range straggling for such ions is large (of the order of the range) the average depth can be controlled very precisely in the 5–200 nm range.

β-NMR Probes at ISAC

At the TRIUMF ISAC facility the primary 500 MeV proton beam is used to produce the radioactive ions. A wide variety of isotopes are released to the surface ionization source heated to 2000°C but alkalis are preferentially ionized because of their low ionization energy. The resulting positive ions are then accelerated to 30 keV forming a low emittance beam with an energy spread of 1–2 eV. The beam is then passed through a high resolution mass spectrometer so that only the isotope of interest reaches the experimental area.

Although any β-emitting nucleus with non-zero spin can be studied with β-NMR, the number of isotopes suitable as a probe in condensed matter is much smaller. The most essential requirements are: (1) a high production efficiency, (2) a method to efficiently polarize the nuclear spins, and (3) a high β-decay asymmetry. Other desirable features are: (4) low mass to reduce radiation damage on implantation, (5) a small value of spin so that the βNMR spectra are relatively simple, and (6) a radioactive lifetime that is not much longer than a few seconds. Table 1 gives a short list of the isotopes we have identified as suitable for development at ISAC where production rates of $10^6/s$ are easily attainable. Our initial efforts have focused on ^{8}Li ($I = 2$), which is the lightest suitable isotope for ?-NMR. The low mass means that the implanted ^{8}Li rests at crystalline sites away from any radiation damage. Also the mean lifetime (1.2s) is comparable to typical nuclear spin relaxation times in many materials. In addition, both the gyromagnetic ratio (γ= 6.3 MHz/T) and electric quadrupole moment of ^{8}Li (Q = +33 mB) are small so that hyperfine interactions with the crystal environment are weak. For example, in metals we expect small metallic frequency shifts in the 100 ppm range;

Table 1: Examples of isotopes suitable for β-NMR. The production rates are projections except in the case of ^{8}Li.

Isotope	Spin	$T_{1/2}$ (s)	γ (MHz/T)	Maximum β-Decay Asymmetry	Production rate (s^{-1})
^{8}Li	2	0.8	6.26	0.33	10^{8}
^{11}Be	1/2	13.8	22	0.33	10^{7}
^{15}O	1/2	122	10.8	0.7	10^{8}
^{17}Ne	1/2	0.1		0.33	10^{6}

whereas, the electric quadrupolar splittings at non-cubic sites should be only 10s of kHz. Thus, with narrow resonances and relaxation rates slow compared to heavier nuclei, we expect that ^{8}Li will act as a high resolution probe of internal magnetic fields in solids. Although the intrinsic resolution determined by the ^{8}Li lifetime and its gyromagnetic ratio is a few mG, the line broadening in solids limits this to about 500 mG. Nevertheless, this is an order of magnitude greater than is possible with muon spin rotation.

Polarized ^{8}Li Beam

Large nuclear polarization of the low energy $^{8}Li^{+}$ beam is created using a fast collinear optical pumping method, which is well-established for the case of alkalis. A schematic of the polarizer at ISAC is shown in Figure 2. Continuous circularly polarized light from a single frequency ring dye laser (300mW power) is directed along the beam axis [10]. The first step in the procedure is to neutralize the ion beam by passing it through a Na vapor cell. The neutral beam then drifts 1.9 m in the optical pumping region in the presence of a small (1 mT) longitudinal magnetic field. The D_1 atomic transition $2s^2S_{1/2} \rightarrow 2p^2P_{1/2}$ of neutral Li occurs at 671 nm. After about 10–20 cycles of absorption and spontaneous emission, a high degree of electronic and nuclear spin polarization is achieved. The final step is to strip off the valence electron by passing it through a He gas cell [11]. The polarized $^{8}Li^{+}$ beam can then be guided electrostatically to one of the spectrometers without affecting the nuclear spin polarization. Typically the polarization of the beam is about 70% and very stable on the time scale of a measurement. The spectrometers are positioned so that the polarization direction is parallel to the high field spectrometer and transverse to the axis of the beam entering the β-NQR spectrometer.

The final electrostatic elements of the beamline are used to focus and steer the beam to the sample. This tuning is achieved by placing a plastic scintillator at the sample position and viewing it with a CCD camera. ^{8}Li decays to ^{8}Be, which in turn promptly decays into two energetic alphas of 1–2 MeV. The resulting light emitted from the scintillator is easy to detect with exposure times of about 1 s. Analysis of the images (see Figure 3) indicates that more than 95% of the beam falls within 4 mm diameter. This defines the

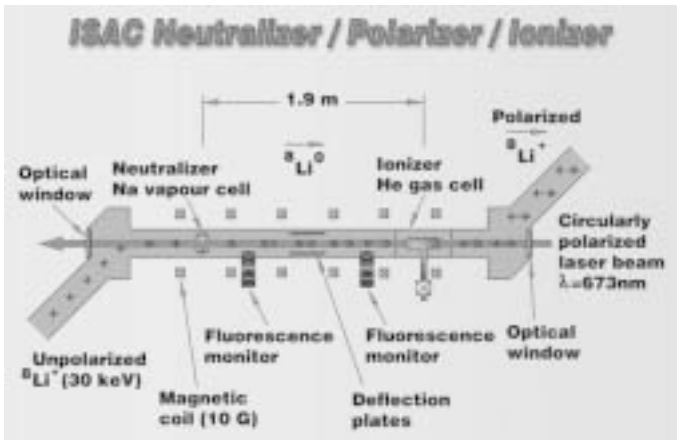

Figure 2. *A schematic of the ISAC polarizer. A 30 keV $^{8}Li^{+}$ ion beam is neutralized in the Na cell and then reionized in the He cell. In the intermediate drift region, a dye laser is used to pump the D1 optical transition of the ^{8}Li atom with circularly polarized light. The resulting polarized ion beam is guided to either the* β*-NQR spectrometer or the high field* β*-NMR spectrometer*

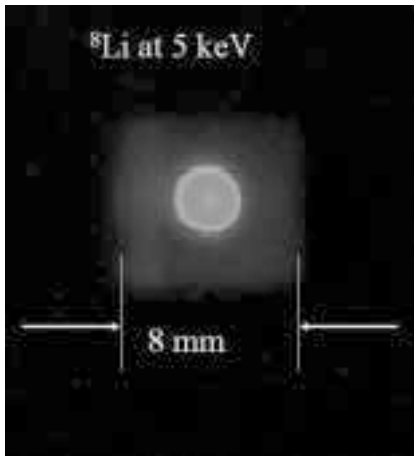

Figure 3. *^{8}Li beamspot image from a small scintillator in the high field spectrometer observed with a CCD camera. More than 95% of the beam is estimated to fall within a 4 mm diameter.*

Figure 4. *A schematic of the high field* β*-NMR spectrometer. The beam passes through a small hole in the B detector and then is focussed onto the sample in the bore of a 9T superconducting solenoid.*

minimum area of a sample that can be studied.

The nominal energy of the beam (30 keV) corresponds to an average implantation depth of about 200 nm. However, the *β*-NMR spectrometer sits on a high voltage platform so that the energy of implantation can be adjusted. Recently we have demonstrated that it is possible to decelerate such a beam down to 84 eV. A similar platform is currently being designed for the *?*-NQR spectrometer. In this way it is possible to measure resonances as a function of implantation depth in the range of 5–200 nm.

Spectrometers

High Field β*-NMR Spectrometer*

A schematic of the spectrometer is shown in Figure 4. The polarized beam enters from the left and passes through a hole in the back detector before entering the last Einzel lens at the entrance to the high-homogeneity 9 T superconducting solenoid. The beam spot at the center of the magnet is a sensitive function of the Einzel lens voltage, magnetic field, and beam energy.

The spectrometer has longitudinal geometry, such that the polarization and magnetic field are both along the beam axis. This is necessary for measurements in high magnetic fields, where both the incoming ions and outgoing betas are strongly focused by the magnet. The forward detector is on the beam/magnet axis and is located several cm downstream of the sample. In order to detect betas in the backward direction (opposite to the beam direction), it is necessary that the detector be outside the magnet because the betas are confined to the magnet axis while inside the magnet bore. Although the solid angles subtended by the two detectors in the zero field are very different, they have similar detection efficiencies in high magnetic fields due to this focusing effect.

The spectrometer and final leg of the beamline are UHV (ultra high vacuum) vacuum compatible in order to avoid a buildup of residual gases on the surface of the sample. Differential pumping is used to reduce the pressure from 10^{-7} torr

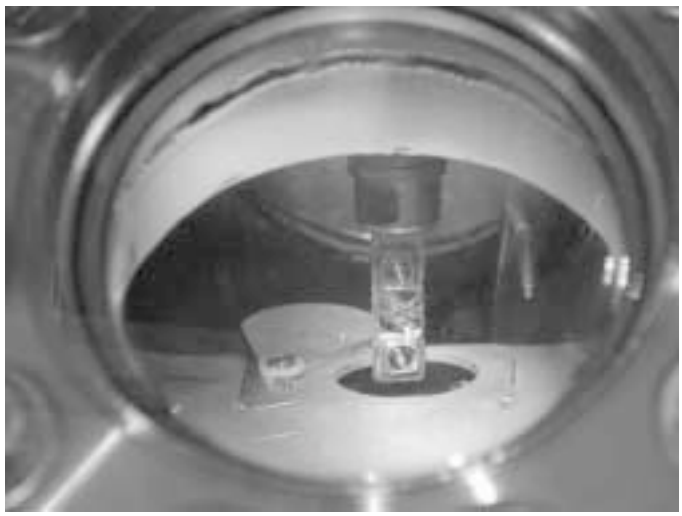

Figure 5. *Photograph of the spectrometer on the high voltage platform. The bellows has been extended so that the sample and cryostat is in the loading position.*

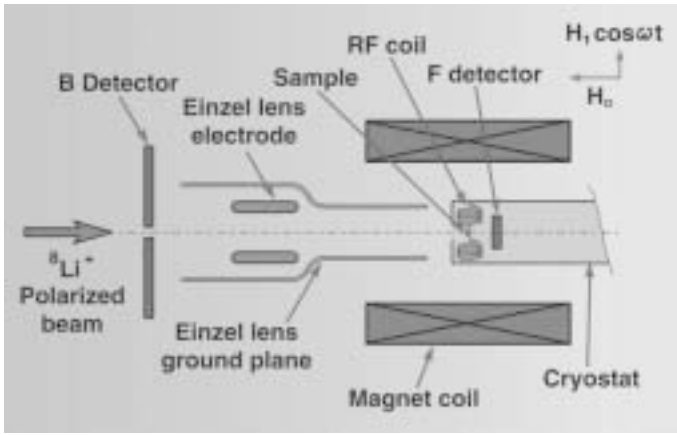

Figure 6. *Photograph of the gold foil being loaded into the UHV vacuum chamber of the high field* β*-NMR spectrometer.*

upstream of the spectrometer to 10^{-10} torr in the main chamber. The sample cryostat is mounted on a large bellows, so that it can be withdrawn from the magnet bore in order to change the sample through a load lock on top of the main vacuum chamber. The photograph in Figure 5 shows the magnet, bellows, and load lock from the back end. Figure 6 shows a gold foil being loaded into the UHV chamber through the lock. Plastic scintillation detectors are used to detect the betas from $^{8}Li \rightarrow {}^{8}Be + \nu_e + e^-$, for which the end point energy is 13 MeV.

β*-NQR spectrometer*

The β-NQR spectrometer is less complicated. The beam enters the ultra high vacuum chamber with initial polarization transverse to the beam direction. The β's pass through thin stainless steel windows and are detected in left and right detectors placed symmetrically on either side of the sample and parallel to the initial polarization direction. A set of three magnetic coils are present that allow one to apply a static uniform magnetic field (0–15 mT) along the initial polarization direction, or to zero the field to within 0.005 mT. The oscillating H_1 field is applied in the vertical direction which is perpendicular to both the beam and polarization direction.

Example Results

β*-NMR in a Ag Film on a MgO Substrate*

Depth profiling with β-NMR was demonstrated by implanting the beam into a 19 nm–thick Ag film grown on a single crystal of MgO. The sample was provided by T. Hibma from the University of Groningen. Figures 7b and 7c shows the resulting β-NMR spectra for two different implantation energies. In Figure 7c the high voltage platform is grounded so that the ^{8}Li stops almost entirely in the MgO substrate. At all temperatures a single narrow line is observed in the MgO. The absence of any quadrupolar splitting indicates that the electric field gradient at the stopping site is almost zero as expected for the tetrahedral interstitial and substitutional sites. The position of the resonance is determined by the applied field because the local

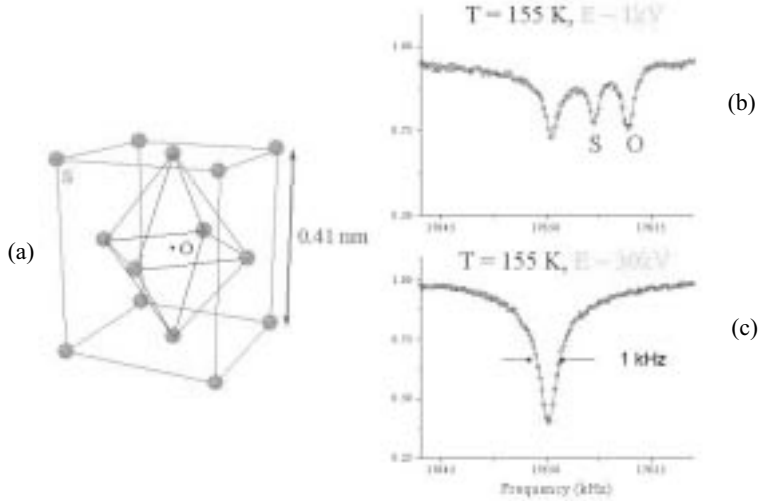

Figure 7. β*-NMR spectra on a 20 nm of epitaxially Ag film on a MgO substrate. In (c) the implantation energy in 30 keV so that the signal comes from the MgO substrate. The resonance position in MgO is determined primarily by the applied magnetic field because it is an insulator and the chemical shifts are only a few ppm. In (b) the energy of implantation is 1 keV so that a significant fraction of the beam stops in the Ag film. The two additional resonances are attributed to Ag where hyperfine coupling to the conduction electrons produces a site-dependent Knight shift. The higher frequency line is attributed to the octahedral interstitial site whereas, the lower frequency line is due to ^{8}Li at a subsitutional site.*

static susceptibility in a non-magnetic insulator is small. The frequency spectrum in Figure 7b is taken with the platform voltage set to 1 keV below the beam energy. In this case most of the beam stops in the Ag film. The residual MgO signal is attributed to part of the beam that lands in an area of the the substrate not covered by the film. Two additional resonances in Figure 7b occur at slightly higher frequencies and are attributed to ^{8}Li in the thin Ag film. Again the absence of quadrupolar splittings imply that both resonances originate from sites with cubic symmetry. The resonances are shifted relative to MgO due to the hyperfine interaction with the conduction electrons of Ag. These metallic "Knight" shifts are on the order of a few hundred ppm as expected for a light ion such as Li. A recent study of these lines as a function of temperature concludes that the higher frequency line comes from ^{8}Li at the octahedral interstitial site (labeled O in Figure 7a), whereas the lower frequency resonance is from the substitutional site [22] (labeled S in Figure 7a). The lines are remarkably sharp, confirming that the implanted Li resides in sites that are well away from any radiation damage.

There are several applications of this result. Because Ag is relatively inert and can be easily evaporated onto any surface, one could use the β-NMR resonance to measure the magnetic field distribution near the surface of a material with a resolution of about 0.5 G. In this way the polarized low energy beam can be used as a kind of local magnetometer. For example, one could use this method to characterize the vortex lattice near the surface of a superconductor. Also, conventional NMR of small metallic particles has revealed interesting but poorly understood confinement effects [18] Such finite size effects may be elucidated by doing β-NMR on thin metal films, wires, or dots.

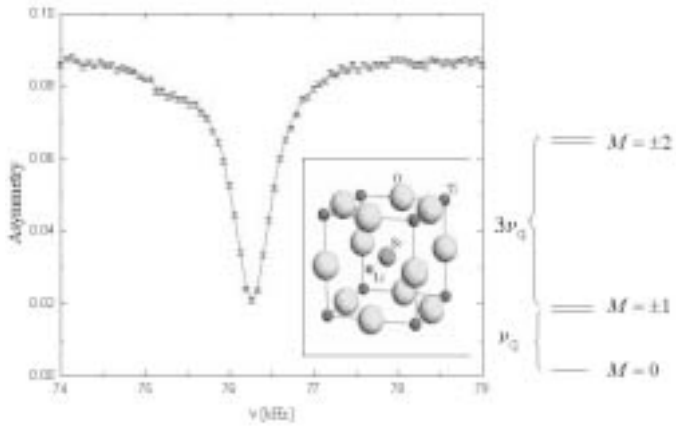

Figure 8. *The ?-NQR spectrum obtained for a $SrTiO_3$ single crystal at room temperature in zero external field. The resonance occurs when the frequency of H_1 equals $3\nu_q$ corresponding to the m=2 to m=1 quadrupolar transition frequency. The inset shows the location of the Li ion at the face center of the cube.*

β-*NQR in* $SrTiO_3$

In many materials the local site symmetry in less than cubic. In this case there is an electric field gradient at the ^{8}Li nucleus that couples to the small electric quadrupole moment of ^{8}Li and produces an energy splitting between the nuclear spin states in the zero magnetic field. This complicates the β-NMR spectrum in an applied field and can lead to many small resonances. However the simplicity is restored in zero applied field where the spin Hamiltonian reduces to:

$$H_q = h\nu_q[I_z^2 - 2] \qquad (2)$$

Here $\nu_q = e^2qQ/8$, $eq = \nu_{zz}$ is the electric field gradient (EFG), Q is the electric quadrupole moment of the nucleus, and $\hat{z}$ is symmetry axis of the EFG tensor. The energy eigenvalues $E_m = h\nu_q(m^2 - 2)$ are a function of the azimuthal quantum number m where $I_z|m\rangle = m|m\rangle$. In the zero applied field there are two resonant frequencies (for $I = 2$) at ν_q and $3\nu_q$ corresponding to the allowed magnetic dipole transitions $0 \leftrightarrow \pm 1$ and $\pm 1 \leftrightarrow \pm 2$, respectively. The amplitude of each resonance is directly proportional to the induced change in the nuclear spin polarization $P_z(\nu)$ on resonance.

Figure 8 shows the β-NQR spectrum taken on a single crystal of $SrTiO_3$, which is a common substrate used in the growth of thin films such as high Tc superconductors. A large resonance occurs at a frequency corresponding to $3\nu_q$. Note that 80% of the polarization is destroyed on resonance. This is about 10 times larger than the amplitude estimated assuming the simple spin Hamiltonian above. This amplification of the resonance can be explained with a slightly non-axial electric field gradient at the Li site, which leads to mixing of the m = ±1 states and causes most of polarization to be destroyed on resonance [23]

β-NQR also has many applications because it can be done in a zero static

applied field. For example one can use it to characterize the superconductivity near the surface or interface of a high Tc superconductor. Under certain circumstances we expect the superconductivity to be different near the surface than in the bulk. Some theories predict a broken time reversal symmetry leading to small magnetic fields that would be evident in the β-NQR spectrum

Summary and Conclusion

We have demonstrated that it is possible to carry out β-detected NMR and β-detected NQR using a beam of low energy, highly polarized $^{8}Li^{+}$. Depth profiling of the signals can be done on a nanometer scale. We anticipate that the technique will have many applications in studies of ultra-thin films, interfaces, and other issues related to electron confinement where it is difficult to obtain equivalent information using conventional NMR.

Acknowledgments

This work was supported by the CIAR, NSERC, and TRIUMF. We also wish to acknowledge many people at TRIUMF who have helped make these experiments possible, especially Don Arseneau, Rick Baartman, Suzanna Daviel, Syd Kreitzman, and Rene Poutissou. We also thank Rahim Abasalti and Bassam Hitti for superb technical support. Finally, we thank Laura Greene for providing the $SrTiO_3$ sample and T. Hibma for the Ag film.

References

1. C. P. Slichter, in *Principles of Magnetic Resonance*, third ed., Springer-Verlag, New York, 1990., pp. 485–500.
2. C. S. Wu et al., *Phys. Rev*., 105, (1957) 1413.
3. R. F. Kiefl et al., *Physica B* 289–290 (2000) 640–647.
4. H. Ackermann, P. Heitjans and H.-J. Stöckmann in *Hyperfine Interactions of Radioactive Nuclei* J. Christiansen, ed., Topics in Current Physics Vol. 31 (Springer, Berlin, 1983), p. 291.
5. P. Heitjans, W. Faber, A. Schirmer, *J. Non-Cryst. Solids* 131 (1991) 1053–1062.
6. B. Ittermann, G. Welker, F. Kroll, F. Mai, K. Marbach, and D. Peters, *Phys. Rev*. B 59 (1999) 2700.
7. T. R. Beals et al., *Physica B* 326 (2003) 205.
8. E. Morezoni, et al *Physica B* 326 (2003) 196.
9. R.F. Kiefl et al., *Physica B* 326 (2003) 189–195.
10. M. Keim, U. Georg, A. Klein, R. Neugart, M. Neuroth, S. Wilbert, P. Lievens, L. Vermeeren, and the ISOLDE Collaboration, *Hyperfine Interactions* 97–98 (1996) 543.
11. C. D. P. Levy et al., *NIM B* 204 (2003) 689–693.
12. M. H. Cohen and F. Reif, Quadrupole Effects in Nuclear Magnetic Resonance Studies of Solids, *Solid State Physics* 5, (1957) 321–438.
13. T. P. Das and E. L. Hahn, *Nuclear Quadrupole Resonance Spectroscopy*, Academic Press Inc. (1958).
14. C. H. Townes and A. L. Schawlow, *Microwave Spectroscopy*, McGraw-Hill Book Company (1955).
15. W. A MacFarlane et al., *Physica B* 326 (2003) 209.
16. W. Körner et al., *Phys. Rev. Lett*., 49 (1982) 1735.
17. Y. Inaguma et al., *J. Electrochem. Soc*., 142 (1995) L8; and *Solid State Ionics* 79 (1995), 91.
18. H. Brom and J. J. van der Klink, *Prog. NMR Spect*. 36, 89 (2000) and references therein.
19. Ch. Niedermayer et al., *Phys. Rev. Lett*., 83 (1999) 3932 .
20. H. Hoffsass and G. Lindner, *Phys. Rep*., 201 (1991) 121.
21. M. Füllgrabe et al., *Phys. Rev., B* 64 224302 (2001) and references therein.
22. G. D. Morris, W. A. MacFarlane, K. H. Chow, R. F. Kiefl, Z. Salman, D. J. Arseneau, A. Hatakeyama, S. R. Kreitzman, C. D. P. Levy, R. Poutissou, R.H. Heffner, J.E. Elenewski, L. H. Greene, submitted to *Phys. Rev. Lett.,* (2003).
23. Z. Salman, E. P. Reynard, W. A. MacFarlane, J. Chakhalian, K. H. Chow, S. Kreitzman, S. Daviel. C. D. P. Levy, R. Poutissou, and R. F. Kiefl, submitted to *Phys. Rev., B* (2003).

R.F. Kiefl
TRIUMF, 4004 Wesbook Mall, Vancouver, BC, Canada, V6T 2A3 and Department of Physics and Astronomy, University of British Columbia, Vancouver, BC, Canada, and Canadian Institute for Advanced Research, Canada

K. H. Chow
Department of Physics, University of Alberta, Edmonton, AB, Canada

W. A. MacFarlane
Departments of Chemistry, University of British Columbia, Vancouver, BC, Canada

G. D. Morris
Los Alamos National Laboratory, K764, Los Alamos, NM 87545, USA

C. D. P. Levy
TRIUMF, 4004 Wesbook Mall, Vancouver, BC, Canada, V6T 2A3

Z. Salman
TRIUMF, 4004 Wesbook Mall, Vancouver, BC, Canada, V6T 2A3

KEK-JAERI Joint RNB facility, TRIAC

Introduction

Research and development on an isotope separator on-line (ISOL)-based radioactive nuclear beam (RNB) facility in Japan had mainly been carried out at the Institute for Nuclear Study (INS), University of Tokyo [1]. The first RNB acceleration was realized with the split-coaxial RFQ (SCRFQ) and interdigital-H (IH) type linacs in March 1997.

A joint RNB facility, TRIAC (Tokai Radioactive Ion Accelerator Complex) facility, is partly based on the re-installation of the above INS-facility in Tokai site of the Japan Atomic Energy Research Institute (JAERI). It will open up the RNB science with 1.1 MeV/u RNBs from FY2005. The higher energetic (5–8 MeV/u) RNBs will be available in the near future.

The facility in a final goal [2] consists of the ISOL, a newly designed charge-breeding electron cyclotron resonance ion-source (CB-ECR), and a linac complex such as the SCRFQ-linac, the IH-linac, three Bunchers, and a superconducting (SC-) linac (see Figure 1). The output energy is variable from 0.1 to 8 MeV/u. Main characteristics of this facility are summarized in Table 1.

The primary protons as well as heavy-ions are supplied from the 20 MV Tandem accelerator to produce radioactive nuclei via the nuclear reactions, namely, nuclear fusions, transfers and fission processes. These radioactive nuclear atoms are ionized and are mass-separated to form low-energy RNBs (2 keV/u). The CB-ECR, which is an ionic charge state converter of the mass-separated RNB from 1^+ to q^+, makes it possible to accelerate heavy radioactive nuclei by the linac complex.

The output energy of IH-linac can be varied from 0.14 MeV/u to 1.09 MeV/u. The low energy RNBs from the IH-linac will be further accelerated by the SC-linac as mentioned in the following section. In order to match the rf-frequency of the SC-linac (130 MHz), ones of the SCRFQ- and the IH-linacs were increased by 2% to 26 MHz and 52 MHz, respectively.

There are two experimental halls. One is for the low-energy (LE-) experiments with 1.1 MeV/u RNBs, and the other is for the high-energy (HE-) experiments with 5–8 MeV/u RNBs. Some experimental devices for nuclear astrophysics and nuclear physics are already placed as mentioned in Ref. [1].

It is noted that another 14 GHz ECR for the production of the stable nuclear beam is also available not only for a tuning of the linac complex, but also for some research subjects with the intense heavy-ion beams independent from Tandem beams.

Based on the results of the RNB developments, the expected beam intensity of ^{143}Cs-RNB is, for example, to be 5×10^5 pps under the realistic condition of the 30 MeV and 3 μA protons and 2.6 g/cm^2 UC-target in the graphite fiber (11 μm$^{\phi}$).

The highest charge breeding efficiencies of the CB-ECR reached to 13.5% for Ar^{9+}, 10.4% for Kr^{12+}, and 6.8% for Xe^{20+}, respectively, at the off-line test [3]. All of these high charge states fulfill the A/q-ratio being less than 7. A charge-breeding time was also measured with using pulsed Xe^{1+}-ions. This quantity is characterized as a delay-time of the extraction of charge-bred q^+-ions from the injection of 1^+-ions and a growth-time of the extracted highly charged ion beam. The measured charge-breeding time was 60 ms for the case of the conversion of $q = 1^+$ to 21^+. This value is enough short with respect to the half-lives of almost all of heavy neutron-rich fission fragments available in TRIAC.

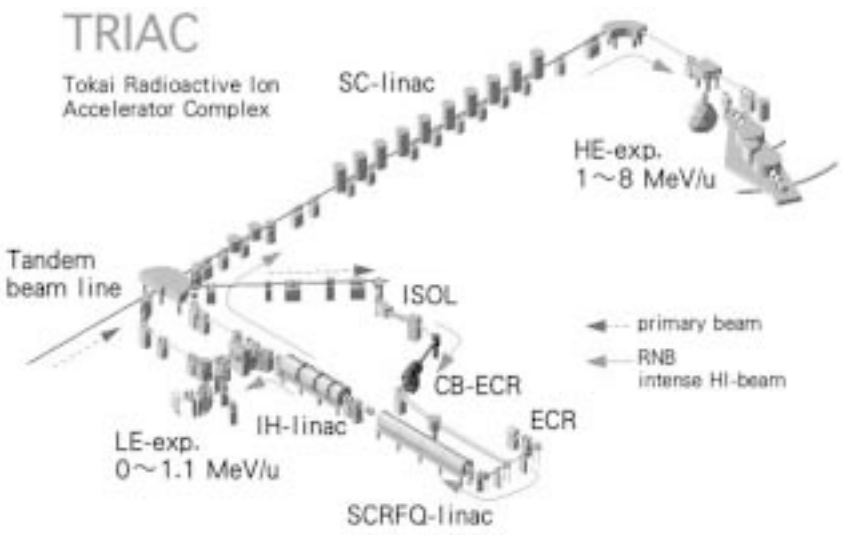

Figure 1. *The layout of TRIAC.*

Table 1. Main Characteristics of TRIAC.

Primary Beam	energy, intensity	40 MeV, p, 3μA, HI (20MV)
Production Target	UC_2, etc	
ISOL	M/ΔM, I/S	1200, FEBIAD, Surface, etc.
Charge Breeder	ECRIS	18 GHz, 1 kW
I/S for stable HI	ECRIS	14 GHz, 200 W
linac complex	injection energy	2.1 keV/u
	output energy	0.14-8.52 MeV/u (variable)
	duty cycle	100% (A/q≤16), 30% (A/q=29)
SCRFQ-linac	frequency, output energy	25.96 MHz, 178.4 keV/u (A/q≤29)
IH-linac	frequency, output energy	51.92 MHz, 0.14-1.09 MeV/u (A/q≤10)
SC-linac*	frequency, output energy	129.8 MHz, < 5.25 MeV/u (A/q≤7), < 8.52 MeV/u (A/q≤4)

*The structure of the SC-linac will be modified from the original one (40 cavities) to the one with 8 low-β cavities + 36 original cavities.

Modification of the SC-Linac

The SC-linac, which was constructed in 1993 as a booster accelerator of the Tandem accelerator, comprises 10 cryostats and inter-cryostat quadrupole doublets. Each cryostat has 4 cavities. The optimum incident velocity is designed to be β = 0.1, which is, however, still high for the output energy of the IH-linac (1.1 MeV/u). Therefore, we will modify the upstream 8 cavities to accept the low-β beams by replacing new ones, each of which will be optimized for the beam velocity of β = 0.06. Moreover, one cryostat including the original 4 cavities will be added to the last cryostat to achieve the higher output energy. The newly designed low-β cavity has 3 acceleration gaps. The expected output energy of the modified SC-linac, consisting of 8 low-β cavities and 36 original cavities, is 5.25 MeV/u for A/q = 7 and 8.52 MeV for A/q = 4. The performance of the modified cryostat with low-β cavities has been tested since this year. All of these modifications will be finished in 2 to 3 years.

Pilot Experiments

At the early stage of the facility, RNBs of 1.1 MeV/u will be available. The interesting research fields with low-energy RNB are solid-state physics, atomic physics and nuclear astrophysics, as well as nuclear physics. Some experimental subjects presently being discussed and preparing are summarized as (1) direct measurements of astrophysical reaction rates, (2) measurements of thermal diffusion constants in materials, (3) spectroscopic studies of exotic nuclei by means of the nuclear spin polarization technique or the Coulomb excitation technique, and (4) studies of electromagnetic structures of materials by means of the PAC-spectroscopy or β-NMR technique.

Some pilot experiments with low-energy RNB have already been performed at JAERI and at TRIUMF. For the experiments at JAERI, RNBs have been obtained by utilizing the inverse transfer reaction and the recoil mass separator in Tandem facility [4].

One of the first subjects is for a direct measurement of the ^{8}Li(α, n) reaction cross section in an energy region from E_{cm} = 0.3 to 2 MeV corresponding to the Gamow peak at T_9 = 1 to 3, which is an important region for the heavy element synthesis in going across the stability gap of A = 8 under the explosive stellar conditions such as an early universe and a supernova explosion.

The ^{8}Li-RNB was produced via the

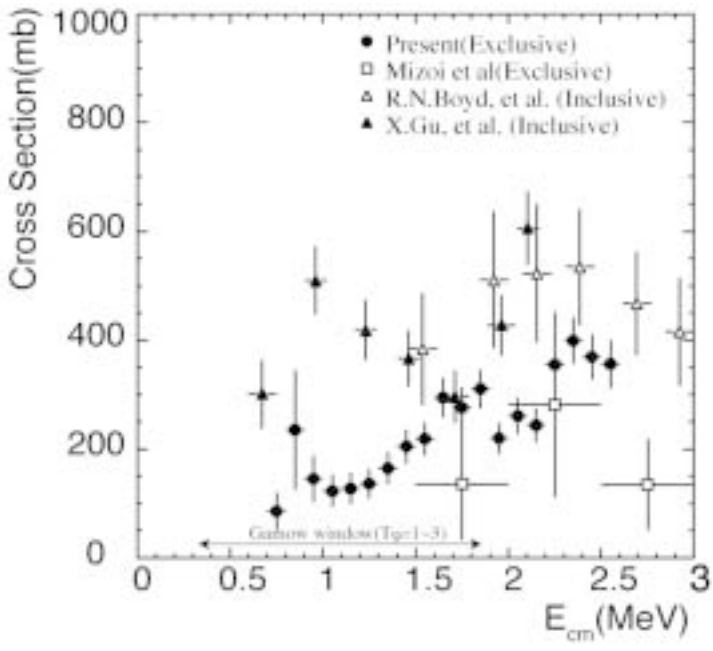

Figure 2. *The reaction cross section of the ^{8}Li(α, n)^{11}B. The open and solid triangles show previous inclusive measurements [5,6], whereas the open squares are the previous exclusive ones [7].*

transfer reaction of ^{9}Be(^{7}Li, ^{8}Li). Its purity and typical beam intensity are 99% and 2×10^{5} pps. In order to overcome such relatively weak beam intensity, we newly constructed a detector system consisting of a large solid angle neutron wall and a 3-dimensional tracking gas chamber. The typical detection efficiency for the ^{8}Li(α, n) reaction events at E_{cm} = 2 MeV is about 15%. The first result obtained in the energy region from E_{cm} = 0.7 to 2.5 MeV has revealed ten times better statistics compared to the previous exclusive measurement as shown in Figure 2 [8]. There is a large discrepancy between our exclusive measurement and the previous inclusive ones. A measurement in the low energy region around 0.5 MeV was also performed. Its analysis is now in progress. A systematic exclusive measurement of (α, n) cross sections for light neutron-rich nuclei is planned at TRIAC.

A pilot experiment of the second subjects is for a non-destructive measurement of a thermal diffusion constant of Li-ion in LiAl intermetallic compound. A new technique to measure the diffusion constants in solids has been developed [9]. In the recent experiment, the energetic (~ 0.5 MeV/u) ^{8}Li has been implanted with the depth of 12 μm into the LiAl compound. The implanted ^{8}Li decays into two α-particles, whose average range in LiAl is 8 μm. Then a charged particle detector, located close to the sample surface, could efficiently detect α-particles from ^{8}Li diffusing toward the sample surface. The time-dependent yields of α-particles are therefore supposed to be a good measure of the Li-diffusion in the sample.

Figure 3 shows the time spectrum of α-particle yield normalized by the time-dependent amount of ^{8}Li-nucleus in LiAl, where a pulsed ^{8}Li-beam was used. The normalized α-particle yields measured at different temperatures (20°C, 150°C, and 300°C) show a clear diffusion effect. The preliminary comparison is also presented with most probable diffusion constants assumed in the one-dimensional simulation based on the Fick's 2nd law, well demonstrating that the present method could be applied for the direct measurement of diffusion constants in a non-destructive way of other methods such as an indirect NMR technique [10]. The method will be extended to measure the Li-ion diffusion constants in the superionic conductors such as electrode materials in Li-batteries in order to study the mechanism of the ionic conductivity.

Finally, one of the third subjects, being in progress at the ISAC facility of TRIUMF under the collaboration of KEK and Osaka University, is to establish the low-lying level scheme of a neutron-rich ^{11}Be through the study of β-delayed neutron emission and γ-decay of the spin-polarized ^{11}Li [11]. This method takes advantage of the discrete nature of the allowed β-decay asymmetry parameter, which is characteristic of the final state spin value.

The ^{11}Li-beam supplied from the ISAC was spin-polarized by the collinear optical pumping. By controlling carefully the line width of a newly installed ring dye-laser system, the spin polarization of about 50% was obtained. The upper panel of Figure 4 shows neutron counts measured as a function of the neutron flight time, and the lower one is the β-decay asymmetry in coincidence with the respective neutrons together with the expected asymmetry values for three possible spin values of ^{11}Be. The neutron peaks 1, 3b, 4, and 10 correspond, for example, to the neutron decays to the

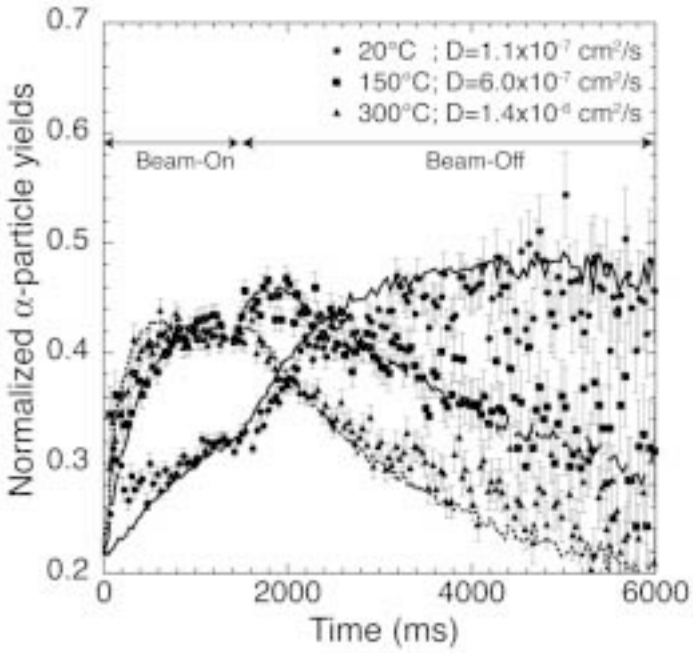

Figure 3. *Normalized time spectra of α-yields at the temperature as indicated in the legend. Solid, dashed, and dotted lines are fitted results with the most probable diffusion constants at 20°C, 150°C, and 300°C, respectively.*

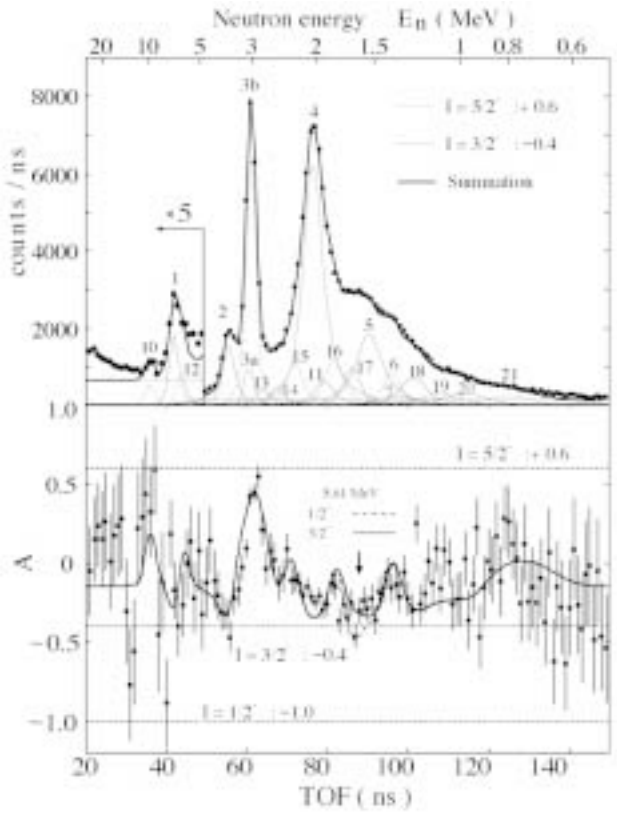

Figure 4. *Neutron TOF spectrum (upper) and β-decay asymmetry parameter (lower) as a function of neutron flight time. Thin curves in the upper figure are resolved neutron transitions and the thick line in the lower figure is the expected asymmetry from the resolved transitions.*

ground state of ^{10}Be. The spin-parity values of the initial states are clearly assigned as $3/2^-$, $5/2^-$, $3/2^-$, and $5/2^-$, respectively. It is interesting to note that some neutron decays that are not clearly seen in the energy spectrum can be observed more clearly in the asymmetry spectrum; one of such examples is a peak around 30 ns. Because this prominent feature could facilitate to decompose overlapping peaks observed in the energy spectrum, we succeeded in the spin-parity assignment of 8 known states in ^{11}Be and solved some problems arising from the contradictory results reported previously. The precise decay spectroscopy by means of the spin-polarized exotic nuclei will be extended for various kinds on nuclear species in TRIAC.

Summary

KEK-IPNS (Institute of Particle and Nuclear Studies) and JAERI-Tokai have been collaborating to construct the RNB facility based on the ISOL and post-acceleration scheme. From FY2005, the low-energy RNBs having its energy up to 1.1 MeV/u will be available for various scientific subjects of nuclear astrophysics, nuclear physics, material science, and related research fields. The higher energy RNBs will be available by replacing some cavities of the SC-linac to newly designed low-β cavities in near future.

In parallel with the developments for TRIAC, some pilot experiments have been also performed, which are (1) direct measurement of ^{8}Li(α, n) reaction rates relevant to the heavy-element synthesis in the astrophysical explosive environments, (2) measurement of the diffusion constants of Li in Li-superionic conductors, and (3) the decay spectroscopy of spin-polarized ^{11}Li. These subjects will be fully performed at TRIAC facility.

References

1. T. Nomura, *Proc. 1st. Int. Conf. Radioactive Nuclear Beams*, California, USA, 16–18 Oct., 1989, World Scientific (1990).
2. H. Miyatake, et al., *Nucl. Instrum. Meth.* B204, 746 (2003).
3. S. C. Jeong et al., *Rev. Sci. Instrum.* 75, 1631 (2004).
4. H. Ishiyama et al., *Proc. Tours Symp.,* AIP 704, 435 (2004).
5. R .N. Boyd et al., *Phys. Rev. Lett*. 68, 1283 (1992).
6. X. Gu et al., *Phys. Lett.* B343, 31 (1995).
7. Y. Mizoi et al., *Phys. Rev.* C62, 065801 (2000).
8. Preliminary results were published in H. Miyatake et al., *Nucl. Phys*. A738, 401 (2004).
9. S. C. Jeong et al., *Jpn. J. Appl. Phys.* 42, 4567 (2003).
10. J. C. Tarczon et al., *Mat. Sci. Eng.* A101, 99 (1988).
11. Y. Hirayama et al., *Nucl. Phys.* A738, 201 (2004).

H. Miyatake
High Energy Accelerator Research Organization (KEK)

H. Ikezoe
Japan Atomic Energy Research Institute (JAERI)

TRIAC Collaboration

International Workshop on Fundamental Interactions

The European Centre for Theoretical Studies in Nuclear Physics and Related Areas (ECT*) in Trento, Italy, hosted the *International Workshop on Fundamental Interactions* from June 21–25, 2004.

In spite of the astounding success the Standard Model (SM) enjoys in describing the strong and electroweak forces, the existence of new fundamental interactions is expected, for several compelling theoretical reasons and especially because of the recent observations of neutrino oscillations. More experimental clues are urgently needed to distinguish among the many proposed speculative SM extensions and to guide new model building. The big accelerator centers of particle physics are not the only arena in which the search for new interactions is being conducted. In fact, nuclear physics facilities, low and intermediate energy, offer unique opportunities to contribute to this quest. NuPECC recognized this in connection with their 2004 long-range plan. Some of the most central and intriguing questions that face the field in the near future, and that are within the realm of nuclear physics, are the following:

- To learn about the nature of the neutrinos, the mixing parameters must be determined and precise measurements of the absolute masses are needed. Double β-decay experiments should be pursued to establish neutrinos being Dirac or Majorana particles.
- Searches for electric dipole moments in different systems (neutron, nuclei, atoms, molecules) have a very high potential to discover new sources of *CP* violation, as required by baryo/leptogenesis models.
- Processes that violate baryon or lepton number or lepton flavor are extremely well suited to constrain speculative SM extensions.
- Correlation measurements in β-decay can reveal non-*V-A* contributions to weak processes.
- Parity nonconservation in atoms and in electron-nucleon scattering.
- Speculations about violation of *CPT* and Lorentz invariance.
- Possible time dependence of fundamental "constants."

At the workshop, ongoing efforts to answer these questions, both theoretically and experimentally, were highlighted and discussed in depth. The workshop was concluded with a discussion to identify urgent future work.

Several experiments that need input from theory were identified. **(1)** The new-physics potential of atomic parity violation experiments needs to be establised. The reliability of the necessary atomic theory must be improved. **(2)** The calculation of Schiff moments of deformed nuclei needs a firmer microscopic basis. **(3)** The relation between forward nuclear scattering and fundamental issues must be firmed up. **(4)** New microscopic approaches to the nuclear matrix elements for 0ν2β experiments are urgently needed. **(5)** The inconsistency in $(g\text{-}2)_\mu^{hadr}$ from e^+e^- and τ-decay data needs to be resolved; the hadronic light-by-light evaluation must be improved. **(6)** Which quantities are relevant to compare in testing CPT invariance?

Similarly, theoretical activities that need experimental confirmation or input were found. **(1)** The Dirac or Majorana nature of neutrinos must be settled. **(2)** The Heidelberg/Moscow 0ν2β experiment suggests Majorana neutrinos; independent confirmation is needed (e.g., the Cuoricino/Cuore experiment) **(3)** Direct mass measurements (e.g., KATRIN) are imperative to fully understand neutrinos. **(4)** Leptonic *CP* violation should be looked for. More precise neutrino oscillation experiments are needed. This research could benefit from a multi-MW proton accelerator, like many others, such as searches for rare decays. **(5)** Experiments to measure the EDM in Radon and Radium are under way. **(6)** A new technique to measure the EDMs of charged particles in a magnetic storage ring has been proposed. The deuteron and the muon will be probed first. **(7)** There are hints from cosmology for a time variation of the fine structure constant a, which needs independent confirmation. **(8)** The implications of this result for other fundamental constants needs to be studied. **(9)** Additional experimental input to $(g\text{-}2)_\mu^{hadr}$ is expected (e.g., KLOE).

Organizers: K. Jungmann, R.G.E. Timmermans (Groningen Univ.), Ch. Weinheimer (Bonn Univ.). Website: http://www.kvi.nl/~trimp/web/html/trento.html. This workshop was financially supported by ECT.

GERCO ONDERWATER
KVI, Groningen

Australian Academy of Science
50th Anniversary
Annual General Meeting 2004
May 5-7, 2004
Senior Award Presentations

Lyle Medal

The Thomas Ranken Lyle medal is awarded no more than every other year, for distinguished Australian Research in Mathematics and Physics. The award was instituted in 1931 by the Australian National Research Council.

The 2003 medal was presented to:

Professor George Dracoulis, *FAA*
Professor of Physics and Head,
Department of Nuclear Physics
Australian National University
Canberra

For research on the structure of atomic nuclei.

CITATION

George Dracoulis has made outstanding contributions to our understanding of the structure of atomic nuclei. His research has been characterized by the development of techniques for the selective formation of nuclei and the determination of their properties. This work has ensured that the nuclear laboratory at the Australian National University has a place among the foremost nuclear structure laboratories in the world.

IBA-Europhysics Prize 2004 for "Applied Nuclear Science and Nuclear Methods in Medicine"

The Executive Committee of the EPS has approved the recommendation of the Nuclear Physics Board according to the proposal of the IBA-EPS prize Selection Committee to award the IBA-Europhysics Prize 2004 to: Professor Guy Demortier, Directeur of LARN (1989–2003) (Laboratoires d'Analyses par Réactions Nucléaires) Facultés Universitaires Notre Dame de la Paix, 61 rue de Bruxelles, B 5000 Namur.

The prize is attributed with the citation: *"For outstanding and innovative research in many and various fields of applied nuclear physics namely in new materials, catalysts, biological material, archaeology and nuclear medicine and, most notably, resulting in ways to improve PET-scans ."*

The prize is sponsored by the IBA (Ion Beam Applications) Executive Committee, Chemin du Cyclotron, 1348 Louvain la Neuve, Belgium. It was delivered during the 8th European Conference on Accelerators in Applied Research and Technology (ECAART 8) in Paris (20–24 September 2004).

Prof. Ch. Leclercq-Willain
President, IBA-EPS Selection Committee,
Université libre de Bruxelles,
B 1050 Bruxelles

Professor Guy Demortier

Lise Meitner Prize for Nuclear Science 2004

The Nuclear Physics Board of the European Physical Society announces the award of the 2004 Lise Meitner Prize for Nuclear Science to Professor Bent Herskind (Neils Bohr Institute, Copenhagen) and Professor Peter Twin (University of Liverpool, UK) for their pioneering development of experimental tools, methods of analysis, and experimental discoveries concerning rapidly spinning nuclei, resulting in particular in the discovery of superdeformed bands. Medals and cheques were presented to the two Laureates at a special ceremony at the International Nuclear Physics Conference, INPC2004, in Goteborg, Sweden on 2nd July 2004.

In the understanding of atomic nuclei, the connection between shell structure and symmetry (as well as spontaneously broken symmetry) has been a central theme. The investigation of rotational motion has been a very fruitful strategy in the study of these issues. In quantum theory the appearance of a rotational mode

Professor Bent Herskind

Professor Peter Twin

demands a deviation from rotational symmetry of the quantum state (deformation), and the best established collective motion in nuclei is rotation. If most of the excitation energy can be concentrated on collective rotational motion the temperature is very low and the internal structure is well ordered. The excitation mechanism has to be carefully chosen in order to realize such highly excited cold nuclei with high spins. One of the surprising experimental discoveries of the 1980s was that nuclei can accommodate a surprisingly large amount of excitation energy in a simple rotational motion when they are created in particular configurations. These configurations are called superdeformed states because then the nucleus has a shape like a Rugby ball with its long axis twice as long as its short axis.

The possibility of superdeformation in nuclei was first proposed in the 1960s as an interpretation of isomeric states observed in actinide nuclei that decay by spontaneous fission rather than gamma-ray emission, which is inhibited by the unusual shape. Shell-structure is associated with the bunching of one-particle levels in the average binding potential, a phenomenon common to quantal many-body systems, and leads to an understanding of how the superdeformed state, and hence isomerism, can occur. It was later realized that because of their large moments of inertia superdeformed states could become the states of lowest energy for a given high spin and be observed at high spins in many other nuclei. The signatures of superdeformed bands are unusually large moments of inertia and strong collectivity, both of which can be pinned down by measuring gamma rays emitted in the decay process. Herskind and Twin were pioneers and key contributors to the development of detector systems and the analysis of emitted gamma rays that identify this novel shape.

Superdeformed states at high spin are created through nuclear reactions between carefully chosen heavy ions that fuse and decay to produce the required species. In the process huge numbers of gamma-rays corresponding to transitions that have nothing to do with superdeformed bands are produced. The challenge is to identify the relevant gamma-rays from this abundance.

The development of large arrays of high-efficiency, high-resolution multi-detector arrays was crucial. In Europe a leading role in this was played by Herskind. Furthermore, Herskind was the leader in the introduction of escape-suppressed Ge detectors for detecting gamma-rays in a coincidence setup. The continuous development of these detector systems in Europe led to the TESSA array, which paved the way for more advanced detector systems like NORDBALL, EUROGAM, EUROBALL, and their descendent, the next generation project AGATA. The HERA detector systems were a parallel development by F.Stephens in Berkeley, USA. The detector array TESSA2, which led to the discovery of superdeformation by Twin, was built at Daresbury Laboratory, building on an earlier collaboration between British and Nordic groups between 1980 and 1982.

In 1986 a band of 19 discrete lines was observed by Twin et al., in 152Dy. The associated gamma-ray lifetimes were so short that the only natural explanation was that the states involved were superdeformed and shaped like a Rugby ball. Within a few years superdeformed bands were identified in other mass regions and a roductive period of nuclear spectroscopy in this new field started. Today, superdeformed rotational bands have been discovered all over the nuclear chart.

The discovery of superdeformed bands opened up a new exciting area of nuclear physics and has had an enormous impact on the whole field of nuclear structure physics with interesting connections to molecular, solid state, and many-body physics. Through Herskind and Twin's outstanding achievements European nuclear structure physics has been able to obtain a frontline position in the scientific world.

Ron C. Johnson
University of Surrey,
Chairman, Nuclear Physics Board